Adv Comput Math (2018) 44:245–275
DOI 10.1007/s10444-017-9542-z

A plane wave method combined with local spectral elements for nonhomogeneous Helmholtz equation and time-harmonic Maxwell equations

Qiya Hu[1,3] · **Long Yuan**[2]

Received: 15 May 2016 / Accepted: 29 May 2017 /
Published online: 9 June 2017

Abstract In this paper we are concerned with plane wave discretizations of nonhomogeneous Helmholtz equation and time-harmonic Maxwell equations. To this end, we design a plane wave method combined with local spectral elements for the discretization of such nonhomogeneous equations. This method contains two steps: we first solve a series of nonhomogeneous local problems on auxiliary smooth subdomains by the spectral element method, and then apply the plane wave method to the discretization of the resulting (locally homogeneous) residue problem on the global solution domain. We derive error estimates of the approximate solutions generated by this method. The numerical results show that the resulting approximate solutions possess high accuracy.

Communicated by: Karsten Urban

The first author was supported by the Natural Science Foundation of China G11571352. The second author was supported by China NSF under the grant 11501529 and Qingdao applied basic research project under the grant 17-1-1-9-jch.

✉ Qiya Hu
hqy@lsec.cc.ac.cn

✉ Long Yuan
yuanlong@lsec.cc.ac.cn

[1] LSEC, Institute of Computational Mathematics and Scientic/Engineering Computing, Academy of Mathematics and Systems Science, Chinese Academy of Sciences, Beijing 100190, China

[2] College of Mathematics and Systems Science, Shan Dong University of Science and Technology, 579 Qian Wan Gang Road, Qingdao 266590, China

[3] University of Chinese Academy of Sciences, Beijing, China

Keywords Helmholtz equation · Time-harmonic Maxwell equations · Nonhomogeneous · Local spectral element · Plane wave basis functions · Error estimates

Mathematics Subject Classification (2010) 65N30 · 65N55

1 Introduction

The plane wave method, which falls into the class of Trefftz methods [31], differs from the traditional finite element method and the boundary element method in the sense that the basis functions are chosen as exact solutions of the governing differential equation without boundary condition. This type of numerical method was first introduced to solve Helmholtz equations. Examples of this approach include the Ultra Weak Variational Formulation (UWVF) (see [5, 7, 8]), the plane wave Lagrangian multiplier (PWLM) method [1, 12, 30], the plane wave discontinuous Galerkin (PWDG) method (see [15, 18]), the weighted plane wave least-squares (PWLS) method (see [21, 26]) and the Variational Theory of Complex Rays (VTCR) introduced in [27, 28]. The wave-based discontinuous Galerkin method was originally proposed in [14] for time-harmonic hyperbolic equations. The plane wave discretization method has been extended to the discretization of time-harmonic Maxwell equations recently (see [19, 22, 23]). The plane wave methods have an important advantage over the other methods for discretizations of Helmholtz equation and time-harmonic Maxwell equations: the resulting approximate solutions have higher accuracies. We would like to point out that the PWLS method and the PWDG method not only can generate high accuracy approximations but also are easy to implement.

Since plane wave basis functions on each element are solutions of the *homogeneous* Helmholtz equation or time-harmonic Maxwell equations without boundary condition, the plane wave methods can not be directly applied to discretizations of the *nonhomogeneous* Helmholtz equation and time-harmonic Maxwell equations. For example, a post-processor is needed in the UWVF method for the discretization of the nonhomogeneous case (refer to [7]). Recently, a PWLS method combined with local finite elements was proposed for the discretization of the nonhomogeneous time-harmonic Maxwell equations (see [22]). The basic ideas in this method can be described as follows: at first nonhomogeneous local problems on every elements are discretized in the space consisting of linear or higher order polynomials, then the resulting residue problem (which is approximately homogeneous on each element) on the global solution domain is discretized by the PWLS method. However the high accuracy merit of the plane wave method can not be kept yet, because the analytic solution of the nonhomogeneous local problem defined on each element (which is a non-smooth domain) has only low regularity even if the analytic solution of the original problem defined on the global solution domain is smooth enough. This phenomenon also appears in the UWVF method for the discretization of nonhomogeneous problems.

Based on the above observation we can amend the method introduced in [22] as follows: for each element we define an auxiliary smooth domain that contains the element as its subdomain and has almost the same size with the element, then we

consider a nonhomogeneous local problem defined on the auxiliary smooth domain instead of the original (non-smooth) element and we solve the nonhomogeneous local problem by the spectral element method. The resulting residue problem (which is approximately homogeneous on each element) on the global solution domain is still solved by the plane wave (PWLS or PWDG) method. We call the new method as "Plane wave method combined with local spectral finite elements". For convenience, we describe and analyze the new method associated with the PWLS method only (the idea and results can be extended to PWDG in the natural manner), and we call the method as PWLS-LSFE method. We prove that the approximate solutions generated by the PWLS-LSFE method possess satisfactory error estimates with high convergence orders.

In order to discretize the non-homogeneous Helmholtz equation by a plane wave-type method, the idea that the solution of the non-homogeneous problem is decomposed into the sum of a particular solution and a solution of the residual homogeneous problem has been considered in some existing works (see [2, 3, 9, 10, 20]), but with different definitions of the particular solution from the present work. The first existing method was developed in [2] and [3], where a particular solution was approximated by a linear combination of the fundamental solutions (MFS) or the plane waves (PWM) with multiple test frequencies, and was obtained by globally solving an algebraic system. As pointed out in [3], the efficiency of this method heavily depends on the choice of test frequencies. The second method was proposed in [9, 10, 20], where only point sources (i.e., the source term is the Dirac function) were considered so that the particular solution can be explicitly expressed as Hankel function.

The paper is organized as follows: In Section 2, we describe the proposed PWLS-LSFE method for nonhomogeneous Helmholtz equation and time-harmonic Maxwell equations. In Section 3, we explain how to discretize the resulting variational problems. In Section 4, we derive the desired error estimates for the approximate solutions. In Section 5, we report some numerical results to confirm the effectiveness of the PWLS-LSFE method.

2 Local-global variational formulation for nonhomogeneous time-harmonic problems

In this section we introduce local-global variational formulations for the nonhomogeneous Helmholtz equation and the second-order system of time-harmonic Maxwell equations.

The considered variational formulations are based on a triangulation of the solution domain. Let Ω be the underlying bounded and connected domain in $\mathbb{R}^n$ ($n = 2, 3$). We assume that the domain Ω is strictly star-shaped (refer to [11]). Let Ω be decomposed into the union of some subdomains in the sense that

$$\overline{\Omega} = \bigcup_{k=1}^{N} \overline{\Omega}_k, \quad \Omega_l \bigcap \Omega_j = \emptyset \quad \text{for } l \neq j,$$

where each Ω_k is star-shaped with respect to a ball (refer to [24]), but it may be not a polygon or polyhedron. Let $\mathcal{T}_h$ denote the triangulation comprising the elements $\{\Omega_k\}$, where h is the mesh width of the triangulation. As usual, we assume that $\mathcal{T}_h$ is quasi-uniform and regular. Define

$$\Gamma_{lj} = \partial\Omega_l \bigcap \partial\Omega_j \quad \text{for } l \neq j$$

and

$$\gamma_k = \overline{\Omega}_k \bigcap \partial\Omega \quad (k = 1, \ldots, N), \quad \gamma = \bigcup_{k=1}^{N} \gamma_k.$$

2.1 The case of Helmholtz equation

Consider the following nonhomogeneous Helmholtz equation which is formalized, normalizing the wave's velocity to 1, by

$$\begin{cases} -\Delta u - \omega^2 u = f \ \text{ in } \quad \Omega, \\ (\partial_{\mathbf{n}} + i\omega)u = g \quad \text{on} \quad \gamma = \partial\Omega. \end{cases} \tag{2.1}$$

The outer normal derivative is referred to as $\partial_{\mathbf{n}}$ and the angular frequency by ω, and $f \in L^2(\Omega)$, $g \in L^2(\gamma)$.

As in [22], the basic idea is to decompose the solution u of (2.1) into

$$u = u^{(1)} + u^{(2)}, \tag{2.2}$$

where $u^{(1)}$ is a particular solution of the first equation in (2.1) (without the primal boundary condition), and $u^{(2)}$ satisfies a locally homogeneous Helmholtz equation. But, in the present paper we design a different manner from [22] to realise such decomposition.

In most applications, the domain Ω is a truncation of an unbounded domain and the problem (2.1) can be regarded as an approximation of a Helmholtz equation in an unbounded domain. Thus the function f is well defined in an unbounded domain. Then, without loss of generality, we assume that the function f is well defined in a slightly large domain containing Ω as its subdomain.

For each element Ω_k, let Ω_k^* be a fictitious domain that has almost the same size of Ω_k and contains Ω_k as its subdomain. Let $u^{(1)} \in L^2(\Omega)$ be defined as $u^{(1)}\,|_{\Omega_k} = u_k^{(1)}\,|_{\Omega_k}$ for each Ω_k, where $u_k^{(1)} \in H^1(\Omega_k^*)$ satisfies the nonhomogeneous *local* Helmholtz equation on the fictitious domain Ω_k^*:

$$\begin{cases} -\Delta u_k^{(1)} - \omega^2 u_k^{(1)} = f \ \text{ in } \quad \Omega_k^* \\ (\partial_{\mathbf{n}_k} + i\omega)u_k^{(1)} = 0 \quad \text{on} \quad \partial\Omega_k^* \end{cases} \quad (k = 1, 2, \ldots, N). \tag{2.3}$$

The variational formulation of (2.3) is to find $u_k^{(1)} \in H^1(\Omega_k^*)$ such that

$$\begin{cases} \displaystyle\int_{\Omega_k^*} (\nabla u_k^{(1)} \cdot \nabla \bar{v}_k - \omega^2 u_k^{(1)} \bar{v}_k) d\mathbf{x} + \int_{\partial\Omega_k^*} i\omega u_k^{(1)} \bar{v}_k d\mathbf{x} = \int_{\Omega_k^*} f \bar{v}_k d\mathbf{x}, \\ \qquad\qquad \forall v_k \in H^1(\Omega_k^*) \ (k = 1, 2, \ldots, N). \end{cases} \tag{2.4}$$

It is easy to see that $u^{(2)} = u - u^{(1)}$ is uniquely determined by the following homogeneous Helmholtz equations of $u_k^{(2)} = u^{(2)}\,|_{\Omega_k}$:

$$-\Delta u_k^{(2)} - \omega^2 u_k^{(2)} = 0 \quad \text{in} \quad \Omega_k \ (k = 1, 2, \ldots, N), \tag{2.5}$$

with the following boundary condition on γ and the interface conditions on Γ_{kj}:

$$\begin{cases} (\partial_{\mathbf{n}} + i\omega)u_k^{(2)} = g - (\partial_{\mathbf{n}} + i\omega)u_k^{(1)} & \text{over} \quad \gamma_k, \\ u_k^{(2)} - u_j^{(2)} = -(u_k^{(1)} - u_j^{(1)}) & \text{over} \quad \Gamma_{kj}, \ (k \neq j; k, j = 1, 2, \cdots, N). \\ \partial_{\mathbf{n}_k} u_k^{(2)} + \partial_{\mathbf{n}_j} u_j^{(2)} = -(\partial_{\mathbf{n}_k} u_k^{(1)} + \partial_{\mathbf{n}_j} u_j^{(1)}) & \text{over} \quad \Gamma_{kj} \end{cases} \tag{2.6}$$

Set

$$V(\mathcal{T}_h) = \{v \in L^2(\Omega);\ \Delta v + \omega^2 v = 0 \ \text{ in each } \ \Omega_k\}.$$

According to the idea of the PWLS method introduced in [26] and [21], the variational problem of Eqs. (2.5)–(2.6) is: to find $u^{(2)} \in V(\mathcal{T}_h)$ such that (refer to [21])

$$\begin{aligned} &\sum_{j\neq k}\left(\alpha\int_{\Gamma_{kj}} (u_k^{(2)} - u_j^{(2)})\cdot\overline{(v_k - v_j)}ds + \beta\int_{\Gamma_{kj}} (\partial_{\mathbf{n}_k} u_k^{(2)} + \partial_{\mathbf{n}_j} u_j^{(2)})\cdot\overline{(\partial_{\mathbf{n}_k} v_k + \partial_{\mathbf{n}_j} v_j)}ds\right) \\ &+ \sum_{k=1}^{N}\int_{\gamma_k} (\partial_{\mathbf{n}_k} + i\omega)u_k^{(2)} \cdot \overline{(\partial_{\mathbf{n}_k} + i\omega)v_k}ds \\ &= -\sum_{j\neq k}\left(\alpha\int_{\Gamma_{kj}} (u_k^{(1)} - u_j^{(1)})\cdot\overline{(v_k - v_j)}ds + \beta\int_{\Gamma_{kj}} (\partial_{\mathbf{n}_k} u_k^{(1)} + \partial_{\mathbf{n}_j} u_j^{(1)})\cdot\overline{(\partial_{\mathbf{n}_k} v_k + \partial_{\mathbf{n}_j} v_j)}ds\right) \\ &+ \sum_{k=1}^{N}\int_{\gamma_k} (g - (\partial_{\mathbf{n}_k} + i\omega)u_k^{(1)}) \cdot \overline{(\partial_{\mathbf{n}_k} + i\omega)v_k}ds, \quad \forall v \in V(\mathcal{T}_h), \end{aligned} \tag{2.7}$$

where α and β are given positive numbers (which will be defined later).

Equivalently, Eq. (2.7) can be written as (refer to [21])

$$\begin{cases} \text{Find } u^{(2)} \in V(\mathcal{T}_h) \ \ s.t. \\ a(u^{(2)}, v) = (\xi,\ v)_V - a(u^{(1)}, v), \quad \forall v \in V(\mathcal{T}_h), \end{cases} \tag{2.8}$$

where $a(\cdot, \cdot)$ denote the sesquilinear form associated with the left side of (2.7) and $\xi \in V(\mathcal{T}_h)$ is defined by Riesz representation theorem applied to the term containing g at the right side of (2.7).

Now we give a reasonable choice of the parameters α and β in (2.7). When the wave number ω is large, the solution $u^{(2)}$ becomes high oscillating, and so the integrals containing the normal derivatives have larger scale than the other integrals. The basic idea for the choice of α and β is to keep the same scale of ω for every terms in the left side of (2.7).

To determine the values of α and β, we investigate the action of the operator $\partial_{\mathbf{n}_k}$ on the discretization space. As we will see, a plane wave basis function can be written as $\phi_l(\mathbf{x}) = e^{i\omega(\mathbf{x}\cdot\boldsymbol{\alpha}_l)}$ with a unit wave propagation direction $\boldsymbol{\alpha}_l$. It is clear that

$$\partial_{\mathbf{n}_k}\phi_l(\mathbf{x}) = i\omega(\boldsymbol{\alpha}_l \cdot \mathbf{n}_k)\phi_l(\mathbf{x}) \quad \text{and} \quad (\partial_{\mathbf{n}_k} + i\omega)\phi_l(\mathbf{x}) = i\omega(\boldsymbol{\alpha}_l \cdot \mathbf{n}_k + 1)\phi_l(\mathbf{x}).$$

Namely, the operator $\partial_{\mathbf{n}_k}$ generates a factor ω. Let $u^{(2)}$ and v be linear combinations of the plane wave basis functions on every element. Then, in the left side of (2.7), the second integral and the third integral contain the factor ω^2, but the first

integral does not contain such a factor. Thus, in order to remove the influence of the factor ω^2, we naturally choose $\alpha = \omega^2$ and $\beta = 1$, such that all the terms in the left side of (2.7) contain the common factor ω^2 (in other words, the three terms are balanced with respect to ω).

2.2 The case of Maxwell equations

Consider the following nonhomogeneous time-harmonic Maxwell equations in a three-dimensional (3D) domain, written as a second-order system of equations (refer to [22]):

$$\begin{cases} \nabla \times (\dfrac{1}{i\omega\mu}\nabla \times \mathbf{E}) + i\omega\varepsilon\mathbf{E} = \mathbf{J} & \text{in} \quad \Omega, \\ -\mathbf{E} \times \mathbf{n} + \dfrac{\sigma}{i\omega\mu}((\nabla \times \mathbf{E}) \times \mathbf{n}) \times \mathbf{n} = \mathbf{g} & \text{on} \quad \gamma. \end{cases} \tag{2.9}$$

Here, $\omega > 0$ is the temporal frequency of the field, and $\mathbf{J} \in L^2(\Omega)^3$, $\mathbf{g} \in L^2_{\mathbf{T}}(\partial\Omega)^3$. The material coefficients ε and μ denote the electric permittivity and magnetic permeability, respectively. The parameter σ is called the conductivity. In particular, if ε is complex valued, then the material is known as an absorbing medium; otherwise the material is called a non-absorbing medium (see [22]).

Similarly to the case of Helmholtz equation, we assume that $\mathbf{J}$ is well defined in a slightly larger domain than Ω, and we decompose the solution $\mathbf{E}$ of the problem (2.9) into $\mathbf{E} = \mathbf{E}^{(1)} + \mathbf{E}^{(2)}$, where $\mathbf{E}^{(1)}$ is a particular solution of the first equation in (2.9) (without the primal boundary condition), and $\mathbf{E}^{(2)}$ locally satisfies homogeneous Maxwell equations.

For each element Ω_k, let Ω_k^* be the fictitious domain described in the last subsection. The particular solution $\mathbf{E}^{(1)} \in (L^2(\Omega))^3$ is defined as $\mathbf{E}^{(1)}\,|_{\Omega_k} = \mathbf{E}_k^{(1)}\,|_{\Omega_k}$ for each Ω_k, where $\mathbf{E}_k^{(1)} \in H(\text{curl}; \Omega_k^*)$ satisfies the nonhomogeneous *local* Maxwell equations on the fictitious domain Ω_k^*:

$$\nabla \times (\frac{1}{i\omega\mu}\nabla \times \mathbf{E}_k^{(1)}) + i\omega\varepsilon\mathbf{E}_k^{(1)} = \mathbf{J} \quad \text{in} \quad \Omega_k^* \ (k = 1, 2, \ldots, N) \tag{2.10}$$

with the homogeneous boundary condition

$$-\mathbf{E}_k^{(1)} \times \mathbf{n} + \frac{\sigma}{i\omega\mu}((\nabla \times \mathbf{E}_k^{(1)}) \times \mathbf{n}) \times \mathbf{n} = 0 \quad \text{on} \quad \partial\Omega_k^*. \tag{2.11}$$

The variational formulation of (2.10)–(2.11) is to find $\mathbf{E}_k^{(1)} \in H(\text{curl}, \Omega_k^*)$ such that

$$\begin{cases} \displaystyle\int_{\Omega_k^*} (\frac{1}{i\omega\mu}\nabla \times \mathbf{E}_k^{(1)} \cdot \nabla \times \bar{\mathbf{F}}_k + \imath\omega\varepsilon\mathbf{E}_k^{(1)} \cdot \bar{\mathbf{F}}_k)d\mathbf{x} + \int_{\partial\Omega_k^*} \frac{1}{\sigma}(\mathbf{E}_k^{(1)} \times \mathbf{n}) \times \mathbf{n} \cdot \bar{\mathbf{F}}_k d\mathbf{x} = \int_{\Omega_k^*} \mathbf{J} \cdot \bar{\mathbf{F}}_k d\mathbf{x}, \\ \forall \mathbf{F}_k \in \mathbf{H}(\text{curl}, \Omega_k^*) \ (k = 1, \ldots, N). \end{cases} \tag{2.12}$$

When $\mathbf{J}$ satisfies $\mathbf{J} \in (L^2(\Omega_k^*))^3$, the variational problem (2.12) possesses a unique solution $\mathbf{E}_k^{(1)} \in H(\text{curl}, \Omega_k^*)$ (see [25, Chap 4]).

Set

$$\mathbf{V}(\mathcal{T}_h) = \{\mathbf{F} \in (L^2(\Omega))^3;\ \nabla \times (\frac{1}{i\omega\mu}\nabla \times \mathbf{F}) + i\omega\varepsilon\mathbf{F} = 0 \ \text{ on each } \Omega_k\}$$

and $\mathbf{F}|_{\Omega_k} = \mathbf{F}_k$ for $\mathbf{F} \in \mathbf{V}(\mathcal{T}_h)$. For ease of notation, define

$$\Phi(\mathbf{F_k}) = \frac{\sigma}{i\omega\mu}((\nabla \times \mathbf{F_k}) \times \mathbf{n_k}) \qquad \text{on} \quad \gamma_k = \partial\Omega_k \cap \gamma$$

and

$$\Psi(\mathbf{F}_k) = \frac{1}{i\omega\mu}(\nabla \times \mathbf{F}_k), \ \text{ on } \Omega_k.$$

For each local interface Γ_{lj} $(l < j)$, we define the jumps on Γ_{lj} as follows (note that $\mathbf{n}_l = -\mathbf{n}_j$):

$$[\![\mathbf{F} \times \mathbf{n}]\!] = \mathbf{F}_l \times \mathbf{n}_l + \mathbf{F}_j \times \mathbf{n}_j \ \text{ and } \ [\![\Psi(\mathbf{F}) \times \mathbf{n}]\!] = \Psi(\mathbf{F}_l) \times \mathbf{n}_l + \Psi(\mathbf{F}_j) \times \mathbf{n}_j. \quad (2.13)$$

It is easy to see that $\mathbf{E}^{(2)} = \mathbf{E} - \mathbf{E}^{(1)}$ is uniquely determined by the following homogeneous Maxwell equations of $\mathbf{E}_k^{(2)}$ $(= \mathbf{E}^{(2)}|_{\Omega_k})$:

$$\nabla \times (\frac{1}{i\omega\mu}\nabla \times \mathbf{E}_k^{(2)}) + i\omega\varepsilon\mathbf{E}_k^{(2)} = 0 \quad \text{in} \quad \Omega_k \ (k = 1, 2, \ldots, N), \qquad (2.14)$$

with the following boundary condition on γ and the interface conditions on Γ_{lj} $(l < j;\ l, j = 1, \ldots, N)$:

$$\begin{cases} -\mathbf{E}^{(2)} \times \mathbf{n} + \frac{\sigma}{i\omega\mu}((\nabla \times \mathbf{E}^{(2)}) \times \mathbf{n}) \times \mathbf{n} \\ = \mathbf{g} + \mathbf{E}^{(1)} \times \mathbf{n} + \frac{\sigma}{i\omega\mu}((\nabla \times \mathbf{E}^{(1)}) \times \mathbf{n}) \times \mathbf{n}, \quad \text{on} \quad \gamma; \\ [\![\mathbf{E}^{(2)} \times \mathbf{n}]\!] = -[\![\mathbf{E}^{(1)} \times \mathbf{n}]\!], \quad \text{on} \quad \Gamma_{lj}; \\ [\![\Psi(\mathbf{E}^{(2)}) \times \mathbf{n}]\!] = -[\![\Psi(\mathbf{E}^{(1)}) \times \mathbf{n}]\!], \quad \text{on} \quad \Gamma_{lj}. \end{cases} \qquad (2.15)$$

The variational problem of Eqs. (2.14)–(2.15) is: to find $\mathbf{E}^{(2)} \in \mathbf{V}(\mathcal{T}_h)$ such that (refer to [22])

$$\begin{aligned} &\sum_{k=1}^{N} \int_{\gamma_k} (-\mathbf{E}_k^{(2)} \times \mathbf{n}_k + \Phi(\mathbf{E}_k^{(2)}) \times \mathbf{n}_k) \cdot \overline{-\mathbf{F}_k \times \mathbf{n}_k + \Phi(\mathbf{F}_k) \times \mathbf{n}_k} ds \\ &+ \sum_{l<j} \left(\int_{\Gamma_{lj}} [\![\mathbf{E}^{(2)} \times \mathbf{n}]\!] \cdot \overline{[\![\mathbf{F} \times \mathbf{n}]\!]}\ ds + \int_{\Gamma_{lj}} [\![\Psi(\mathbf{E}^{(2)}) \times \mathbf{n}]\!] \cdot \overline{[\![\Psi(\mathbf{F}) \times \mathbf{n}]\!]}\ ds \right) \\ = &-\sum_{k=1}^{N} \int_{\gamma_k} (-\mathbf{E}_k^{(1)} \times \mathbf{n}_k + \Phi(\mathbf{E}_k^{(1)}) \times \mathbf{n}_k - \mathbf{g}) \cdot \overline{-\mathbf{F}_k \times \mathbf{n}_k + \Phi(\mathbf{F}_k) \times \mathbf{n}_k} ds \\ &-\sum_{l<j} \left(\int_{\Gamma_{lj}} [\![\mathbf{E}^{(1)} \times \mathbf{n}]\!] \cdot \overline{[\![\mathbf{F} \times \mathbf{n}]\!]}\ ds + \int_{\Gamma_{lj}} [\![\Psi(\mathbf{E}^{(1)}) \times \mathbf{n}]\!] \cdot \overline{[\![\Psi(\mathbf{F}) \times \mathbf{n}]\!]}\ ds \right), \ \forall\, \mathbf{F} \in \mathbf{V}(\mathcal{T}_h). \end{aligned} \qquad (2.16)$$

By the definitions of the functions $\Phi(\cdot)$ and $\Psi(\cdot)$, the left side of (2.16) has no factor containing ω when $\mathbf{E}^{(2)}$ and $\mathbf{F}$ are linear combinations of the plane wave basis functions on every element (refer to the discussions at the end of Section 2.1).

Equivalently, Eq. (2.16) can be written as (see [22])

$$\begin{cases} \text{Find } \mathbf{E}^{(2)} \in \mathbf{V}(\mathcal{T}_h) \ \ s.t. \\ A(\mathbf{E}^{(2)}, \mathbf{F}) = (\xi, \ \mathbf{F})_{\mathbf{V}} - A(\mathbf{E}^{(1)}, \mathbf{F}) \quad \forall \mathbf{F} \in \mathbf{V}(\mathcal{T}_h). \end{cases} \tag{2.17}$$

Remark 2.1 We would like to explain the motive to introduce the fictitious domains $\{\Omega_k^*\}$. It is certain that we can choose Ω_k^* as Ω_k itself for each k (see [22] for the details). But, such choice of Ω_k^* has a drawback: since the boundary of each Ω_k is not smooth, the solutions $u^{(1)}$ and $\mathbf{E}^{(1)}$ of the nonhomogeneous local equations (2.3) and (2.10) with $\Omega_k^* = \Omega_k$ have only low regularity even if the known functions f and $\mathbf{J}$ are sufficiently smooth, which implies that the solutions $u^{(2)}$ and $\mathbf{E}^{(2)}$ of the residue homogeneous equations (2.5)–(2.6) and (2.14)–(2.15) may possess low regularity only. This means that the plane wave approximate solutions of the variational problems (2.7) and (2.16) have only low accuracy. Because of this, we choose each fictitious domain Ω_k^* so that it possesses sufficiently smooth boundary $\partial\Omega_k^*$. A natural way is to choose Ω_k^* as the disc (for the two-dimensional case) or the sphere (for the three-dimensional case) that has the same center O_k as Ω_k and has the radius $r_k = \max_r\{dist(O_k, \ V_k^r)\}$, where V_k^r denotes a vertex of Ω_k. Notice that the center O_k and the radius r_k can be calculated easily.

3 Discretization of the variational problems

In this section we introduce discretizations of the variational problems described in the last section.

3.1 Spectral element discretization of the nonhomogeneous local problems

Since Ω_k^* is a sufficiently smooth domain and f (and $\mathbf{J}$) is smooth on Ω_k^*, the solution $u_k^{(1)}$ (and $\mathbf{E}_k^{(1)}$) possesses high regularity on Ω_k^*. Moreover, the fictitious domain Ω_k^* has almost the same size as the element Ω_k. Thus the subproblems (2.4) and (2.12) should be discretized by the spectral element method, so that the resulting approximate solutions have higher accuracy.

Let q be a positive integer and D be a bounded and connected domain in $\mathbb{R}^n$. Let $S_q(D)$ denote the set of polynomials defined on D, whose orders are less than or equal to q. Set $\mathbf{S}_q(D) = (S_q(D))^3$.

The discrete variational problems of (2.4) are: find $u_{k,h}^{(1)} \in S_q(\Omega_k^*)$ such that

$$\begin{cases} \displaystyle\int_{\Omega_k^*} (\nabla u_{k,h}^{(1)} \cdot \nabla \bar{v}_k - \omega^2 u_{k,h}^{(1)} \bar{v}_k) d\mathbf{x} + \int_{\partial\Omega_k^*} i\omega u_{k,h}^{(1)} \bar{v}_k d\mathbf{x} = \int_{\Omega_k^*} f \bar{v}_k d\mathbf{x}, \\ \qquad\qquad \forall v_k \in S_q(\Omega_k^*) \ (k = 1, 2, \ldots, N). \end{cases} \tag{3.1}$$

Similarly, the discrete variational problems of (2.12) are: find $\mathbf{E}_{k,h}^{(1)} \in \mathbf{S}_q(\Omega_k^*)$ such that

$$\begin{cases} \int_{\Omega_k^*} (\frac{1}{i\omega\mu} \nabla \times \mathbf{E}_{k,h}^{(1)} \cdot \nabla \times \bar{\mathbf{F}}_k + i\omega\varepsilon \mathbf{E}_{k,h}^{(1)} \cdot \bar{\mathbf{F}}_k) d\mathbf{x} + \int_{\partial\Omega_k^*} \frac{1}{\sigma} (\mathbf{E}_{k,h}^{(1)} \times \mathbf{n}) \times \mathbf{n} \cdot \bar{\mathbf{F}}_k d\mathbf{x} = \int_{\Omega_k^*} \mathbf{J} \cdot \bar{\mathbf{F}}_k d\mathbf{x}, \\ \forall \mathbf{F}_k \in \mathbf{S}_q(\Omega_k^*) \ (k = 1, 2, \ldots, N). \end{cases} \tag{3.2}$$

In this paper we choose the fictitious domain Ω_k^* to be the disc (for the two-dimensional case) or the sphere (for the three-dimensional case) described in Remark 2.1. Then the variational problems (3.1) and (3.2) can be solved easily by using the polar coordinate transformation for the calculation of the involved integrations. We would like to emphasize that the discrete problems (3.1) (and (3.2)) are local and independent each other for $k = 1, \cdots, N$, so they can be solved in parallel and the cost is very small.

Define $u_h^{(1)} \in \prod_{k=1}^N S_q(\Omega_k)$ by $u_h^{(1)}|_{\Omega_k} = u_{k,h}^{(1)}|_{\Omega_k}$. Similarly, define $\mathbf{E}_h^{(1)} \in \prod_{k=1}^N \mathbf{S}_q(\Omega_k)$ by $\mathbf{E}_h^{(1)}|_{\Omega_k} = \mathbf{E}_{k,h}^{(1)}|_{\Omega_k}$.

3.2 The plane wave basis function spaces

The discretization is based on a finite-dimensional space $V_p(\mathcal{T}_h) \subset V(\mathcal{T}_h)$. In this subsection, we first give the precise definition of such a space $V_p(\mathcal{T}_h)$.

3.2.1 The case of Helmholtz equation

Let p be a given positive integer. For each element Ω_k, we define p functions y_{kl} $(l = 1, 2, \cdots, p)$ as independent solutions of the homogeneous Helmholtz equation (without boundary condition) in the element Ω_k $(k = 1, 2, \cdots, N)$.

For simplification, we consider some constant number p of basis functions for every elements Ω_k. Particularly, in this paper we will choose y_{kl} as the wave shape functions on Ω_k, which satisfy

$$\begin{cases} y_{kl}(\mathbf{x}) = e^{i\omega(\mathbf{x}\cdot\boldsymbol{\alpha}_l)}, \quad \mathbf{x} \in \Omega_k, \\ \boldsymbol{\alpha}_l \cdot \boldsymbol{\alpha}_l = 1, \\ l \neq s \rightarrow \boldsymbol{\alpha}_l \neq \boldsymbol{\alpha}_s, \end{cases} \tag{3.3}$$

where $\boldsymbol{\alpha}_l$ $(l = 1, \cdots, p)$ are unit wave propagation directions to be specified later.

The basis functions of $V_p(\mathcal{T}_h)$ can be defined as

$$\phi_{kl}(\mathbf{x}) = \begin{cases} y_{kl}(\mathbf{x}), & \text{if } \mathbf{x} \in \Omega_k, \\ 0, & \text{if } \mathbf{x} \in \Omega_j \ \text{(for each } j \neq k) \end{cases} \quad (k = 1, \cdots, N; \ l = 1, \cdots, p). \tag{3.4}$$

Thus the space $V(\mathcal{T}_h)$ is discretized by the subspace

$$V_p(\mathcal{T}_h) = \text{span}\left\{\phi_{kl} : \ k = 1, \cdots, N; \ l = 1, \cdots, p\right\}. \tag{3.5}$$

During numerical simulations, the direction vectors α_l in the wave functions $y_{kl}(\mathbf{x})$, for two-dimensional problems, are uniformly distributed as follows:

$$\boldsymbol{\alpha_l} = \begin{pmatrix} cos(2\pi(l-1)/p) \\ sin(2\pi(l-1)/p) \end{pmatrix} \quad (l = 1, \cdots, p).$$

For three-dimensional problems, we use the optimal spherical codes from [29] to generate the wave propagation directions $\boldsymbol{\alpha_l}$ $(l = 1, \cdots, p)$.

3.2.2 The case of Maxwell equations

In practice, following [6], a suitable family of plane waves, which are solutions of the constant-coefficient Maxwell equations, are defined by choosing p unit propagation directions $\mathbf{d}_l$ (which is generated by the optimal spherical codes from [29]) and p real unit polarization vectors $\mathbf{G}_l$ orthogonal to $\mathbf{d}_l$ $(l = 1, \cdots, p)$. By using such propagation directions and polarization vectors, we can define the complex polarization vectors $\mathbf{F}_l$ and $\mathbf{F}_{l+p}$ as

$$\mathbf{F}_l = \mathbf{G}_l + \mathrm{i}\mathbf{G}_l \times \mathbf{d}_l, \quad \mathbf{F}_{l+p} = \mathbf{G}_l - \mathrm{i}\mathbf{G}_l \times \mathbf{d}_l \quad (l = 1, \cdots, p).$$

Notice that the complex polarization vectors are the same as in [8, 23], but differ slightly from those in [19]. We then define the complex functions $\mathbf{E}_l$:

$$\mathbf{E}_l = \sqrt{\mu}\, \mathbf{F}_l \exp(\mathrm{i}\kappa \mathbf{d}_l^* \cdot \mathbf{x}) \quad (l = 1, \cdots, 2p), \tag{3.6}$$

where $\mathbf{d}_l^* = \mathbf{d}_l$ when $l = 1, \cdots, p$ and $\mathbf{d}_l^* = \mathbf{d}_{l-p}$ when $l = p+1, \cdots, 2p$. It is easy to verify that every function $\mathbf{E}_l$ $(l = 1, \cdots, 2p)$ satisfies the second-order homogeneous Maxwell equation.

Let $\mathcal{Q}_{2p}$ denote the space spanned by the $2p$ plane wave functions $\mathbf{E}_l$ $(l = 1, \cdots, 2p)$. Define the plane wave space

$$\mathbf{V}_p(\mathcal{T}_h) = \left\{\mathbf{v} \in L^2(\Omega) : \ \mathbf{v}|_K \in \mathcal{Q}_{2p} \ \text{ for any } \ K \in \mathcal{T}_h\right\}. \tag{3.7}$$

It is clear that the above space has $N \times 2p$ basis functions, which are given by

$$\phi_l^k(\mathbf{x}) = \begin{cases} \mathbf{E}_l(\mathbf{x}), & \text{if } \mathbf{x} \in \Omega_k, \\ 0, & \text{if } \mathbf{x} \in \Omega_j \ (\text{for each } \ j \neq k) \end{cases} \quad (k = 1, \cdots, N; \ l = 1, \cdots, 2p). \tag{3.8}$$

3.3 Discrete variational formulations of the homogeneous problems defined on the global domain

With the finite-dimensional plane wave space $V_p(\mathcal{T}_h) \subset V(\mathcal{T}_h)$, the discrete variational problem of Eq. (2.8) can be described as follows:

$$\begin{cases} \text{Find } u_h^{(2)} \in V_p(\mathcal{T}_h) \quad s.t. \\ a(u_h^{(2)}, v_h) = (\xi, \ v_h)_V - a(u_h^{(1)}, v_h), \quad \forall v_h \in V_p(\mathcal{T}_h). \end{cases} \tag{3.9}$$

The discrete variational problem associated with Eq. (2.17) can be described as follows:

$$\begin{cases} \text{Find } \mathbf{E}_h^{(2)} \in \mathbf{V}_p(\mathcal{T}_h) \quad s.t. \\ A(\mathbf{E}_h^{(2)}, \mathbf{F}_h) = (\xi,\ \mathbf{F}_h)_{\mathbf{V}} - A(\mathbf{E}_h^{(1)}, \mathbf{F}_h), \quad \forall \mathbf{F}_h \in \mathbf{V}_p(\mathcal{T}_h). \end{cases} \tag{3.10}$$

It is clear that $a(v, v) \geq 0$. Moreover, it can be verified directly that, for $v \in V(\mathcal{T}_h)$, $a(v, v) = 0$ if and only if $v = 0$ (some details can be found in [21]). Thus $a(v, v)$ is a norm on $V(\mathcal{T}_h)$ and so the problem (3.9) is uniquely solvable. Similarly, $A(\mathbf{F}, \mathbf{F})$ is a norm on $\mathbf{V}(\mathcal{T}_h)$ and the problem (3.10) is uniquely solvable (refer to [22]).

Define $u_h = u_h^{(1)} + u_h^{(2)}$ and $\mathbf{E}_h = \mathbf{E}_h^{(1)} + \mathbf{E}_h^{(2)}$. Then u_h and $\mathbf{E}_h$ are the desired approximations of u and $\mathbf{E}$, respectively.

4 Error estimates of the approximate solutions

In this section, we derive error estimates of the approximate solutions u_h and $\mathbf{E}_h$ defined in the previous section.

In the rest of this paper, for a positive integer j and a bounded and connected domain D, let $||v||_{j,D}$ and $|v|_{j,D}$ denote the norm and the semi-norm of v on the Sobolev space $H^j(D)$, respectively. For convergence, let $|v|_{0,D}$ denote the L^2 norm of v on D. As in [24], define the $\omega-$weighted Sobolev norm $||\cdot||_{s,\omega,D}$ as

$$||v||_{s,\omega,D} = (\sum_{j=0}^{s} \omega^{2(s-j)} |v|_{j,D}^2)^{\frac{1}{2}}.$$

4.1 The case of Helmholtz equations

Let $||\cdot||_V$ be the energy norm induced by the sesquilinear form $a(\cdot,\cdot)$ (some explanations are given in Section 3.3), namely,

$$\begin{aligned} ||v||_V^2 = & \sum_{k=1}^{N} \int_{\gamma_k} |(\partial_{\mathbf{n}} + i\omega) v_k|^2 ds \\ & + \sum_{j \neq k} \left(\alpha \int_{\Gamma_{kj}} |v_k - v_j|^2 ds + \beta \int_{\Gamma_{kj}} |\partial_{\mathbf{n}_k} v_k + \partial_{\mathbf{n}_j} v_j|^2 ds \right), \quad v \in V(\mathcal{T}_h). \end{aligned}$$

Since $u = u^{(1)} + u^{(2)}$ and $u_h = u_h^{(1)} + u_h^{(2)}$, we have

$$||u - u_h||_V \leq ||u^{(1)} - u_h^{(1)}||_V + ||u^{(2)} - u_h^{(2)}||_V. \tag{4.1}$$

It suffices to establish estimates of the two terms in the right side of (4.1).

4.1.1 Error estimate of the local spectral element approximations

In this subsubsection, we derive an estimate of $||u^{(1)} - u_h^{(1)}||_V$.

Throughout this paper we assume that each Ω_k^* is a disc or a sphere, whose radius and center are denoted by r_k and O_k respectively. According to the explanations in Remark 2.1, the radius r_k satisfies $c_0 h \le r_k \le C_0 h$. Hereafter, c_0 and C_0 denote two constants independent of ω, h, p and q. In general we assume that $c_0 \le C_0$ in one place, but they may have different values in different places.

In the following discussion, we will use a smoothness assumption of f on each Ω_k^*. But the domain Ω_k^* is not contained in Ω when the element Ω_k adjoins $\partial\Omega$, so we need to know whether f is smooth in a larger domain than Ω.

For a *small* positive number δ, let Ω_δ be the union of Ω and the boundary layer with the thickness δ, i.e.,

$$\Omega_\delta = \Omega \cup \{\mathbf{x} : \ dist(\mathbf{x}, \partial\Omega) < \delta\} = \{\mathbf{x} : \ dist(\mathbf{x}, \Omega) \le \delta\}.$$

Choose δ such that

$$\Omega_\delta \supseteq \cup_{k=1}^N \Omega_k^* = \Omega \cup (\cup_{k\in\Lambda_\partial} (\Omega_k^* \backslash \Omega)),$$

where

$$\Lambda_\partial = \{k; \ \Omega_k \text{ adjoins } \partial\Omega\}.$$

As pointed out in Section 2.1, in most applications the domain Ω is a truncation of an unbounded domain $\tilde{\Omega}$. In theory, the smoothness of the analytic solution u in Ω depends on the smoothness of f in the global domain $\tilde{\Omega}$ and the regularity of the boundary data g on $\partial\Omega$. Since we only study the situation that u is sufficiently smooth in Ω, we can naturally assume that f is smooth enough in Ω_δ.

We would like to point out that the domain Ω_δ is only slightly larger than Ω since the size of each $\Omega_k^* \backslash \Omega$ is very small. Thus, even if the domain Ω is not a truncation of an unbounded domain, the assumption is still very weak.

We first give a stability result of $u_k^{(1)}$ for each k.

Lemma 4.1 *Assume that $c_0 \le h\omega \le C_0$ and $f \in H^{s-2}(\Omega_k^*)$ with an integer $s \ge 2$. Let $u_k^{(1)}$ denote the solution of the nonhomogeneous local equation (2.3). Then $u_k^{(1)} \in H^s(\Omega_k^*)$ and*

$$|u_k^{(1)}|_{s,\Omega_k^*} \le C \sum_{r=0}^{s-2} \omega^{s-r-2} ||f||_{r,\Omega_k^*}. \tag{4.2}$$

Proof Define the scaling transformation $\hat{\mathbf{x}} = F_k(\mathbf{x}) = r_k^{-1}(\mathbf{x} - O_k) + O_k$. We use the scaling transformation $\hat{\mathbf{x}} = F_k(\mathbf{x})$ to map Ω_k^* to a disc ($2d$ case) or a sphere ($3d$ case) with the radius 1, which is denoted by $\hat{D}_k$. The image of $u_k^{(1)}(\mathbf{x})$ is denoted by $\hat{u}_k^{(1)}(\hat{\mathbf{x}})$. Set $\hat{\omega}_k = r_k\omega$. Then the equation (2.3) becomes

$$\begin{cases} -\hat{\Delta}\hat{u}_k^{(1)} - \hat{\omega}_k^2 \hat{u}_k^{(1)} = r_k^2 \hat{f} & \text{in} \quad \hat{D}_k \\ (\hat{\partial}_{\mathbf{n}_k} + i\hat{\omega}_k)\hat{u}_k^{(1)} = 0 & \text{on} \quad \partial\hat{D}_k. \end{cases} \tag{4.3}$$

From the assumption, we have $c_0 \le \hat{\omega}_k \le C_0$. By the smoothness assumption of f and the existing regularity results (see, for example, Lemma 3.3 in [11]), we know that $\hat{u}_k^{(1)} \in H^s(\hat{D}_k)$ and

$$|\hat{u}_k^{(1)}|_{s,\hat{D}_k} \le C \sum_{r=0}^{s-2} \hat{\omega}_k^{s-2-r} ||r_k^2 \hat{f}||_{r,\hat{D}_k}. \tag{4.4}$$

Now we use the integral transformation $\hat{\mathbf{x}} = F_k(\mathbf{x})$ to (4.4), and we get the desired results. □

Remark 4.1 If we directly use the existing results (see, for example, [17])), we can only obtain a weaker result that the coefficient in the front of $||f||_{0,\Omega_k^*}$ is ω^{s-1}. Thus the estimate in (4.2) is better than that in the existing results. Here we have used the condition $c_0 \le h\omega \le C_0$. The condition $h\omega \le C_0$ is standard for the discretization of Helmholtz equation and time-harmonic Maxwell equations, otherwise, the resulting approximations may be not convergent.

However, it is unclear whether the assumption $c_0 \le h\omega$ is indeed necessary for the estimate (4.2) since fast convergence of the proposed method still kept when $h \to 0$ (for a fixed ω). We observe that, at least in the case with nonsingular solutions, for the plane wave method (and the spectral element method) for the considered equations, increasing the number p of basis functions on every element is more efficient than decreasing the mesh size h to get approximate solutions with high accuracy. This means that we do not hope to choose a very small mesh size h in applications, provided that the approximation has a satisfactory accuracy. As we will see, for the proposed method the approximation has a satisfactory accuracy when $h\omega \ge c_0$, so we need not to choose a smaller h (we can simply choose $h \approx 1/\omega$). Thus, the assumption $h\omega \ge c_0$ is not a limit in applications.

The following result gives estimates of the local spectral element approximations $u_{k,h}^{(1)}$ $(k = 1, \cdots, N)$.

Lemma 4.2 *Let $q \ge 2$ and $2 \le s \le q+1$. Under the assumptions in Lemma 4.1, we have for each Ω_k^**

$$||u_k^{(1)} - u_{k,h}^{(1)}||_{j,\Omega_k^*} \le C h^{s-j} q^{-(s-j)} |u_k^{(1)}|_{s,\Omega_k^*} \quad (j = 0, 1, 2). \tag{4.5}$$

Proof We use the same notation as that in the proof of the above Lemma. Under the scaling transformation $\hat{\mathbf{x}} = F_k(\mathbf{x})$, the variational problems (2.4) and (3.1) become

$$\begin{cases} \displaystyle\int_{\hat{D}_k} (\nabla \hat{u}_k^{(1)} \cdot \nabla \bar{v} - \hat{\omega}_k^2 \hat{u}_k^{(1)} \bar{v}) d\hat{\mathbf{x}} + i\hat{\omega}_k \int_{\partial \hat{D}_k} \hat{u}_k^{(1)} \bar{v} d\hat{\mathbf{x}} = r_k^2 \int_{\hat{D}_k} \hat{f} \bar{v} d\hat{\mathbf{x}}, \\ \qquad\qquad \forall v \in H^1(\hat{D}_k) \ (k = 1, 2, \ldots, N) \end{cases} \tag{4.6}$$

and

$$\begin{cases} \displaystyle\int_{\hat{D}_k} (\nabla \hat{u}_{k,h}^{(1)} \cdot \nabla \bar{v} - \hat{\omega}_k^2 \hat{u}_{k,h}^{(1)} \bar{v}) d\hat{\mathbf{x}} + i\hat{\omega}_k \int_{\partial \hat{D}_k} \hat{u}_{k,h}^{(1)} \bar{v} d\hat{\mathbf{x}} = r_k^2 \int_{\hat{D}_k} \hat{f} \bar{v} d\hat{\mathbf{x}}, \\ \qquad\qquad \forall v \in S_q(\hat{D}_k)\ (k = 1, 2, \ldots, N), \end{cases} \tag{4.7}$$

respectively. We first derive an error estimate of $\hat{u}_k^{(1)} - \hat{u}_{k,h}^{(1)}$ based on the framework introduced in [13]. Let $\hat{P}_q : H^1(\hat{D}_k) \to S_q(\hat{D}_k)$ denote the orthogonal projector associated with the complex inner product

$$\int_{\hat{D}_k} \nabla v \cdot \nabla \bar{w} d\hat{\mathbf{x}} + i\hat{\omega}_k \int_{\partial \hat{D}_k} v \bar{w} d\hat{\mathbf{x}}, \quad v, w \in H^1(\hat{D}_k).$$

Then $\hat{P}_q \hat{u}_k^{(1)}$ satisfies

$$\begin{aligned} &\int_{\hat{D}_k} \nabla(\hat{P}_q \hat{u}_k^{(1)}) \cdot \nabla \bar{w} d\hat{\mathbf{x}} + i\hat{\omega}_k \int_{\partial \hat{D}_k} (\hat{P}_q \hat{u}_k^{(1)}) \bar{w} d\hat{\mathbf{x}} \\ &= \int_{\hat{D}_k} \nabla \hat{u}_k^{(1)} \cdot \nabla \bar{w} d\hat{\mathbf{x}} + i\hat{\omega}_k \int_{\partial \hat{D}_k} \hat{u}_k^{(1)} \bar{w} d\hat{\mathbf{x}}, \quad \forall w \in S_q(\hat{D}_k). \end{aligned} \tag{4.8}$$

By the approximation of the spectral element method (see, for example, [16]), there is function $\hat{v}_q \in S_q(\hat{D}_k)$ such that

$$||\hat{u}_k^{(1)} - \hat{v}_q||_{j,\hat{D}_k} \le C q^{-(s-j)} |\hat{u}_k^{(1)}|_{s,\hat{D}_k} \quad (j = 0, 1, 2). \tag{4.9}$$

Then, by the standard technique, we can show that

$$||\hat{P}_q \hat{u}_k^{(1)} - \hat{u}_k^{(1)}||_{j,\hat{D}_k} \le C q^{-(s-j)} |\hat{u}_k^{(1)}|_{s,\hat{D}_k} \quad (j = 0, 1). \tag{4.10}$$

Set $\xi = \hat{P}_q \hat{u}_k^{(1)} - \hat{u}_k^{(1)}$ and $\eta = \hat{u}_{k,h}^{(1)} - \hat{P}_q \hat{u}_k^{(1)}$. Combining (4.7) with (4.8), we know that the function $\eta \in S_q(\hat{D}_k)$ is the solution of the following variational problem (see [13])

$$\int_{\hat{D}_k} (\nabla \eta \cdot \nabla \bar{w} - \hat{\omega}_k^2 \eta \bar{w}) d\hat{\mathbf{x}} + i\hat{\omega}_k \int_{\partial \hat{D}_k} \eta \bar{w} d\hat{\mathbf{x}} = \hat{\omega}_k^2 \int_{\hat{D}_k} \xi \bar{w} d\hat{\mathbf{x}}, \quad \forall w \in S_q(\hat{D}_k). \tag{4.11}$$

Thus, by the stability result given in Proposition 3.3 of [17], we have

$$\hat{\omega}_k ||\eta||_{0,\hat{D}_k} + |\eta|_{1,\hat{D}_k} \le C \hat{\omega}_k^2 ||\xi||_{0,\hat{D}_k}.$$

This, together with (4.10), leads to

$$||\eta||_{1,\hat{D}_k} \le C \hat{\omega}_k q^{-s} ||\hat{u}_k^{(1)}||_{s,\hat{D}_k}.$$

Notice that

$$\hat{u}_k^{(1)} - \hat{u}_{k,h}^{(1)} = (\hat{u}_k^{(1)} - \hat{P}_q \hat{u}_k^{(1)}) + (\hat{P}_q \hat{u}_k^{(1)} - \hat{u}_{k,h}^{(1)}).$$

Using (4.10) again, we further get

$$||\hat{u}_k^{(1)} - \hat{u}_{k,h}^{(1)}||_{j,\hat{D}_k} \le C q^{-(s-j)} |\hat{u}_k^{(1)}|_{s,\hat{D}_k} \quad (j = 0, 1). \tag{4.12}$$

Making the integral transformation $\hat{\mathbf{x}} = F_k(\mathbf{x})$ to (4.12), we can deduce that

$$||u_k^{(1)} - u_{k,h}^{(1)}||_{j,\Omega_k^*} \le C r_k^{s-j} q^{-(s-j)} |u_k^{(1)}|_{s,\Omega_k^*} \le C h^{s-j} q^{-(s-j)} |u_k^{(1)}|_{s,\Omega_k^*} \quad (j = 0, 1). \tag{4.13}$$

Here we have used the fact that $r_k = O(h)$.

On the other hand, it follows by (4.9) that

$$||u_k^{(1)} - v_q||_{j,\Omega_k^*} \le C h^{s-j} q^{-(s-j)} |u_k^{(1)}|_{s,\Omega_k^*} \quad (j = 1, 2). \tag{4.14}$$

By the triangle inequality, we have

$$|u_k^{(1)} - u_{k,h}^{(1)}|_{2,\Omega_k^*} \le |u_k^{(1)} - v_q|_{2,\Omega_k^*} + |v_q - u_{k,h}^{(1)}|_{2,\Omega_k^*}. \tag{4.15}$$

Applying the inverse estimate to the second term in the right side of the above inequality, leads to

$$\begin{aligned} |v_q - u_{k,h}^{(1)}|_{2,\Omega_k^*} &\le C q h^{-1} ||v_q - u_{k,h}^{(1)}||_{1,\Omega_k^*} \\ &= C q h^{-1} (||u_k^{(1)} - v_q||_{1,\Omega_k^*} + ||u_k^{(1)} - u_{k,h}^{(1)}||_{1,\Omega_k^*}). \end{aligned}$$

Substituting this into (4.15), and using (4.14) and (4.13), yields

$$|u_k^{(1)} - u_{k,h}^{(1)}|_{2,\Omega_k^*} \le C h^{s-2} q^{-(s-2)} |u_k^{(1)}|_{s,\Omega_k^*}.$$

This, together with (4.13), gives the desired result (4.5). □

Combining Lemma 4.1 with Lemma 4.2, we can derive error estimates of the approximation $u_h^{(1)}$ easily.

Theorem 4.3 *Let $q \ge 2$ and $2 \le s \le q + 1$. Assume that $c_0 \le h\omega \le C_0$ and $f \in H^{s-2}(\Omega_\delta)$. Then the following error estimates hold*

$$\left(\sum_{k=1}^{N} ||u^{(1)} - u_h^{(1)}||_{j,\Omega_k}^2\right)^{\frac{1}{2}} \le C \left(\frac{h}{q}\right)^{s-j} \sum_{l=0}^{s-2} \omega^{s-l-2} ||f||_{l,\Omega_\delta} \quad (j = 0, 1, 2) \tag{4.16}$$

and

$$||u^{(1)} - u_h^{(1)}||_V \le C \left(1 + \frac{\omega^2 h^2}{q^2}\right)^{\frac{1}{2}} \left(\frac{h}{q}\right)^{s-\frac{3}{2}} \sum_{l=0}^{s-2} \omega^{s-l-2} ||f||_{l,\Omega_\delta}. \tag{4.17}$$

Proof By the definitions of $u^{(1)}$ and $u_h^{(1)}$, the estimate (4.16) is a direct result of Lemmas 4.1 and 4.2. In the following we consider the inequality (4.17).

For each element $K \in \mathcal{T}_h$, we have the well known ϵ-inequality, which can be derived by the trace inequality (Theorem 1.6.6 in [4])

$$||w||_{0,\partial K} \le C(\epsilon^{-1} ||w||_{0,K} + \epsilon |w|_{1,K}), \quad w \in H^1(K) \quad (\epsilon \in (0, 1)).$$

Then

$$||u_k^{(1)} - u_{k,h}^{(1)}||_{0,\partial\Omega_k}^2 \le C(h^{-1} q ||u_k^{(1)} - u_{k,h}^{(1)}||_{0,\Omega_k}^2 + h q^{-1} |u_k^{(1)} - u_{k,h}^{(1)}|_{1,\Omega_k}^2)$$

and

$$||\partial_{\mathbf{n}}(u_k^{(1)} - u_{k,h}^{(1)})||_{0,\partial\Omega_k}^2 \le C(h^{-1}q|u_k^{(1)} - u_{k,h}^{(1)}|_{1,\Omega_k}^2 + hq^{-1}|u_k^{(1)} - u_{k,h}^{(1)}|_{2,\Omega_k}^2).$$

Plugging (4.5) in the above two inequalities, leads to

$$||u_k^{(1)} - u_{k,h}^{(1)}||_{0,\partial\Omega_k}^2 \le Ch^{2s-1}q^{-(2s-1)}|u_k^{(1)}|_{s,\Omega_k^*}^2$$

and

$$||\partial_{\mathbf{n}}(u_k^{(1)} - u_{k,h}^{(1)})||_{0,\partial\Omega_k}^2 \le Ch^{2s-3}q^{-(2s-3)}|u_k^{(1)}|_{s,\Omega_k^*}^2.$$

Using the definition of the norm $||\cdot||_V$, and summing the above two inequalities over all the elements, we obtain (refer to [21])

$$\begin{aligned} ||u^{(1)} - u_h^{(1)}||_V^2 &\le C\sum_{k=1}^{N}(\omega^2||u_k^{(1)} - u_{k,h}^{(1)}||_{0,\partial\Omega_k}^2 + ||\partial_{\mathbf{n}}(u_k^{(1)} - u_{k,h}^{(1)})||_{0,\partial\Omega_k}^2) \\ &\le C\sum_{k=1}^{N}(\omega^2h^{2s-1}q^{-(2s-1)} + h^{2s-3}q^{-(2s-3)})|u_k^{(1)}|_{s,\Omega_k^*}^2. \end{aligned}$$

This, together with (4.2), gives the desired result (4.17). □

4.1.2 Error estimate of the plane wave approximations

Let s and m be given positive integers satisfying (see [24]) $m \ge 2(s-1)+1 = 2s-1$. Let the number p of plane wave propagation directions be chosen as $p = 2m+1$ in 2D and $p = (m+1)^2$ in 3D, respectively. In Section 2.1, we have assume that each element Ω_k is star-shaped with respect to a ball.

The following approximate result holds thanks to Corollary 5.5 in [24] (for ease of notation, we only give a simplified form of the result)

Lemma 4.4 *Let $2 \le s \le \frac{m+1}{2}$ with a sufficiently large m. Assume that $\omega h \le C_0$ and $w \in V(\mathcal{T}_h)$ satisfies $w|_{\Omega_k} \in H^s(\Omega_k)$ for each k. Then there is a function $Q_h w \in V_p(\mathcal{T}_h)$ such that*

$$||w - Q_h w||_{j,\Omega_k} \le Ch^{s-j}m^{-\lambda(s-j-\varepsilon)}||w||_{s,\omega,\Omega_k} \quad (0 \le j \le s; k = 1, \cdots, N), \tag{4.18}$$

where $\lambda > 0$ is a constant depending only on the shape of the elements (in particular, $\lambda = 1$ in two dimensions and for convex elements), and $\varepsilon = \varepsilon(m) > 0$ satisfies $\varepsilon(m) \to 0$ when $m \to \infty$.

For ease of notation, in the rest of the paper we set

$$\mathcal{F}(u, f, s) = ||u||_{s,\omega,\Omega} + \sum_{l=0}^{s-2}\omega^{s-l-2}||f||_{l,\Omega_\delta}.$$

Theorem 4.5 *Let $q \geq 2$ and $2 \leq s \leq \min\{\frac{m+1}{2}, q+1\}$. Assume that $c_0 \leq \omega h \leq C_0$, $f \in H^{s-2}(\Omega_\delta)$ and $u \in H^s(\Omega)$. Then*

$$||u^{(2)} - u_h^{(2)}||_V,\ ||u - u_h||_V \leq Ch^{s-\frac{3}{2}} \left(m^{-\lambda(s-1-\varepsilon)+\frac{\delta_\lambda}{2}} + \theta q^{-(s-\frac{3}{2})} \right) \mathcal{F}(u, f, s), \tag{4.19}$$

where $\delta_\lambda = \max\{2\lambda - 1, 1\}$, θ is a positive constant.

Proof From (2.8) and (3.9), we have

$$a(u^{(2)} - u_h^{(2)}, v_h) = a(u_h^{(1)} - u^{(1)}, v_h), \quad \forall v_h \in V_p(\mathcal{T}_h). \tag{4.20}$$

Let Q_h be the operator defined in Lemma 4.4. It follows by (4.20) that

$$a(u^{(2)} - u_h^{(2)}, Q_h u^{(2)} - u_h^{(2)}) = a(u_h^{(1)} - u^{(1)}, Q_h u^{(2)} - u_h^{(2)}).$$

Then, by the direct manipulation, we can deduce that

$$\begin{aligned} a(u^{(2)} - u_h^{(2)}, u^{(2)} - u_h^{(2)}) = {} & a(u^{(1)} - u_h^{(1)}, u^{(2)} - Q_h u^{(2)}) + a(u^{(2)} - u_h^{(2)}, u^{(2)} - Q_h u^{(2)}) \\ & + a(u^{(1)} - u_h^{(1)}, u_h^{(2)} - u^{(2)}). \end{aligned}$$

Furthermore, we obtain

$$||u^{(2)} - u_h^{(2)}||_V^2 \leq (\epsilon_h^{(1)} + \epsilon_h^{(2)})||u^{(2)} - u_h^{(2)}||_V + \epsilon_h^{(1)} \cdot \epsilon_h^{(2)}, \tag{4.21}$$

where

$$\epsilon_h^{(1)} = ||u^{(1)} - u_h^{(1)}||_V \ \text{ and } \ \epsilon_h^{(2)} = ||u^{(2)} - Q_h u^{(2)}||_V.$$

It can be verified directly by (4.21) that

$$||u^{(2)} - u_h^{(2)}||_V \leq \frac{\sqrt{2}+1}{2}(\epsilon_h^{(1)} + \epsilon_h^{(2)}). \tag{4.22}$$

Notice that $u^{(2)}|_{\Omega_k} = (u - u^{(1)})|_{\Omega_k}$. By the assumptions and Lemma 4.1, we have $u^{(2)}|_{\Omega_k} \in H^s(\Omega_k)$ for each k. As in the proof of Theorem 4.3, by (4.18) and (4.2) we can show that

$$\begin{aligned} ||u^{(2)} - Q_h u^{(2)}||_V^2 &\leq C \sum_{k=1}^{N} \left(\omega^2 ||u^{(2)} - Q_h u^{(2)}||_{0,\partial\Omega_k}^2 + ||\partial_{\mathbf{n}}(u^{(2)} - Q_h u^{(2)})||_{0,\partial\Omega_k}^2 \right) \\ &\leq C \sum_{k=1}^{N} \left(\omega^2 h^{2s-1} m^{-2\lambda(s-\varepsilon)+\delta_\lambda} + h^{2s-3} m^{-2\lambda(s-1-\varepsilon)+\delta_\lambda} \right) ||u^{(2)}||_{s,\omega,\Omega_k}^2 \\ &\leq C(1 + (\frac{\omega h}{m^\lambda})^2) h^{2s-3} m^{-2\lambda(s-1-\varepsilon)+\delta_\lambda} \left(||u||_{s,\omega,\Omega}^2 + \sum_{l=0}^{s-2} \omega^{2(s-l)} ||f||_{s,\Omega_\delta}^2 \right) \\ &\leq C_1 h^{2s-3} m^{-2\lambda(s-1-\varepsilon)+\delta_\lambda} \left(||u||_{s,\omega,\Omega}^2 + \sum_{l=0}^{s-2} \omega^{2(s-l)} ||f||_{s,\Omega_\delta}^2 \right). \end{aligned}$$

Substituting (4.17) and the above inequality into (4.22), yields

$$||u^{(2)} - u_h^{(2)}||_V \leq h^{s-\frac{3}{2}} \left(C_1 m^{-\lambda(s-1-\varepsilon)+\frac{\delta_\lambda}{2}} + C_2 q^{-(s-\frac{3}{2})} \right) \mathcal{F}(u, f, s). \tag{4.23}$$

This, together with (4.17), gives the desired result (4.19) (choosing $\theta = 2C_2/C_1$). □

4.1.3 L^2 estimate of the approximations u_h

Based on the discussions in the last two subsubsections, we can obtain the final result easily.

Theorem 4.6 *Let $q \geq 2$ and $2 \leq s \leq \min\{\frac{m+1}{2}, q+1\}$. Assume that $c_0 \leq \omega h \leq C_0$, $f \in H^{s-2}(\Omega_\delta)$ and $u \in H^s(\Omega)$. Then*

$$||u - u_h||_{0,\Omega} \leq C h^{s-2} \omega^{-1} (1 + h\omega) \left(m^{-\lambda(s-1-\varepsilon)+\frac{\delta_\lambda}{2}} + \theta q^{-(s-\frac{3}{2})} \right) \mathcal{F}(u, f, s). \tag{4.24}$$

Proof By the triangle inequality, we have

$$||u - u_h||_{0,\Omega} \leq ||u^{(1)} - u_h^{(1)}||_{0,\Omega} + ||u^{(2)} - u_h^{(2)}||_{0,\Omega}. \tag{4.25}$$

Notice that the triangulation $\mathcal{T}_h$ is quasi-uniform, as in the proof of Lemma 3.7 in [18], we can show the following Poincare-type inequality

$$||w||_{0,\Omega} \leq C \mathrm{diam}(\Omega)(h^{1/2}\omega^{1/2} + h^{-1/2}\omega^{-1/2})\omega^{-1/2}||w||_V, \quad \forall w \in V(\mathcal{T}_h). \tag{4.26}$$

Since $u^{(2)},\ u_h^{(2)} \in V(\mathcal{T}_h)$, we further get

$$||u^{(2)} - u_h^{(2)}||_{0,\Omega} \leq C(1 + \omega h)\omega^{-1} h^{-1/2} ||u^{(2)} - u_h^{(2)}||_V. \tag{4.27}$$

Plugging (4.23) in this inequality, leads to

$$||u^{(2)} - u_h^{(2)}||_{0,\Omega} \leq C(1 + \omega h) h^{s-2} \omega^{-1} \left(m^{-\lambda(s-1-\varepsilon)+\frac{\delta_\lambda}{2}} + \theta q^{-(s-\frac{3}{2})} \right) \mathcal{F}(u, f, s). \tag{4.28}$$

Combing (4.25) with (4.16) and (4.28), yields

$$||u - u_h||_{0,\Omega} \leq C \left(h^s q^{-s} + h^{s-2} \omega^{-1} (1 + \omega h)(m^{-\lambda(s-1-\varepsilon)+\frac{\delta_\lambda}{2}} + \theta q^{-(s-\frac{3}{2})}) \right) \mathcal{F}(u, f, s), \tag{4.29}$$

which implies (4.24). □

Remark 4.2 As pointed out in [24], if we do not care about the dependence of the estimate (4.18) on the number m and we only hope to obtain a h-estimate with optimal order, it is enough to require $2 \leq s \leq m+1$ in Lemma 4.4. This means that the parameter s in Theorem 4.5 and Theorem 4.6 can be chosen as $2 \leq s \leq \min\{m+1, q+1\}$ to get h-estimates with the optimal order.

Remark 4.3 The only difference between Theorem 4.5-Theorem 4.6 and the existing results for homogeneous Helmholtz equations (see [18] and [21]) is that the estimates

(4.19) and (4.24) contain the error term $\theta q^{-(s-\frac{3}{2})}$ of the spectral approximations for the nonhomogeneous local problems.

Remark 4.4 In order to obtain an approximate solution with high accuracy but without superfluous cost, the values of the parameters m (or p) and q should satisfy some balance relations.

We first consider the V-norm error (4.19). We hope that

$$m^{-\lambda(s-1-\varepsilon)+\frac{\delta_\lambda}{2}} \approx \theta q^{-(s-\frac{3}{2})}.$$

For example, when every Ω_k is a convex element in two dimensions, we have $\lambda = 1$ and $\delta_\lambda = 1$, and so

$$m^{-\lambda(s-1-\varepsilon)+\frac{\delta_\lambda}{2}} = m^{-(s-\frac{3}{2}-\varepsilon(m))} \to m^{-(s-\frac{3}{2})}$$

when $m \to +\infty$. Of course, for a fixed m, we have $\varepsilon(m) > 0$, i.e.,

$$m^{-(s-\frac{3}{2}-\varepsilon(m))} > m^{-(s-\frac{3}{2})}.$$

Then we should choose the parameters (m, q) such that the value $m^{-(s-\frac{3}{2})}$ is slightly smaller than the value $\theta q^{-(s-\frac{3}{2})}$, i.e., $m > \theta^{-(s-\frac{3}{2})^{-1}} q$.

When $\theta = 1$, we can choose $m > q$, for example, $m = q + 1$; if $\theta < 1$, then m should be much greater than q; if $\theta > 1$, we may choose $m = q$.

In particular, for a large number s, we have $\theta^{-(s-\frac{3}{2})^{-1}} \to 1$, which implies $m = q + 1$ for a large number s (its necessary condition is that q is large). The numerical results in Section 5 indicate that the parameter m can be roughly chosen as $m = q+2$ or $m = q + 3$, i.e., the direction number $p = 2q + 5$ or $p = 2q + 7$, so that the resulting approximate solutions possess satisfactory accuracies but without extra cost. It can be inferred from the numerical results that the constant $\theta < 1$.

We point out that we are not able to give a unified optimal relation between m and q in theory, since the estimate (4.19) only gives a upper bound of the V-norm error and the value of the constant θ is unknown.

As to the L^2-norm errors, the situation is similar but is a bit different. It is known that the plane wave method has higher order convergence than the spectral element method. Since m and q define the degrees of freedom of the plane wave method and the spectral element method respectively, we can choose $m \approx q$. The numerical results in Section 5 indicate that m should be chosen as an integer in the range $q-1 \le m \le q + 1$, i.e, the direction number p is an odd number in the range $2q - 1 \le p \le 2q + 3$. Similarly, for the case of three dimensions, we can choose $m = q + 1$, i.e., the direction number $p = (q + 2)^2$. As in the case of V-norm errors, we are not able to give a unified optimal balance relation.

4.2 The case of Maxwell equations

Error estimates for the case of Maxwell's equations can be built as in the previous subsection, so we will omit the details and only give the main results.

Let $||\cdot||_{\mathbf{V}}$ be the energy norm induced by the sesquilinear form $A(\cdot,\cdot)$.

The following result can be proved as in Theorem 4.3 (using Lemma 4.1 and Lemma 4.2)

Theorem 4.7 *Under the assumptions in Theorem 4.3 (replacing f with $\boldsymbol{J}$), we have*

$$||\boldsymbol{E}^{(1)} - \boldsymbol{E}_h^{(1)}||_{j,\Omega} \leq C(\frac{h}{q})^{s-j} \sum_{l=0}^{s-2} \omega^{s-l-2} ||\boldsymbol{J}||_{l,\Omega_\delta} \quad (j = 0, 1, 2) \tag{4.30}$$

and

$$||\boldsymbol{E}^{(1)} - \boldsymbol{E}_h^{(1)}||_{\boldsymbol{V}} \leq C(1 + \frac{\omega^2 h^2}{q^2})^{\frac{1}{2}} (\frac{h}{q})^{s-\frac{3}{2}} \sum_{l=0}^{s-2} \omega^{s-l-2} ||\boldsymbol{J}||_{l,\Omega_\delta}. \tag{4.31}$$

Assume that the mesh triangulation $\mathcal{T}_h$ satisfies the definition stated in Ref. [19, Section 5] and set $\lambda = \min_{K\in\mathcal{T}_h} \lambda_K$, where λ_K is the positive parameter that depends only on the shape of an element K of $\mathcal{T}_h$ introduced in Ref. [24, Th. 3.2]. Let s and m be given positive integers satisfying $m \geq 2(s-1)+1$ and $m \geq 2(1+2^{1/\lambda})$. Let the number p of plane wave propagation directions be chosen as $p = (m+1)^2$.

By Theorem 5.4 of [19] and Theorem 4.7, we can derive the following result as in the proof of Theorem 4.5 (refer to Theorem 4.3 in [21]).

Theorem 4.8 *Let s, m, q, h and ω satisfy the assumptions in Theorem 4.5. Assume that $\boldsymbol{J} \in H^{s-2}(\Omega_\delta)$ and $\boldsymbol{E} \in H^s(curl;\Omega)$. Then*

$$||\boldsymbol{E}^{(2)} - \boldsymbol{E}_h^{(2)}||_V,\ ||\boldsymbol{E} - \boldsymbol{E}_h||_V \leq Ch^{s-\frac{3}{2}}(\omega^{-1} m^{-\lambda(s-\frac{5}{2})} + q^{-(s-\frac{3}{2})}) \mathcal{F}(\nabla\times\boldsymbol{E}, \boldsymbol{J}, s). \tag{4.32}$$

Remark 4.5 Notice that the conditions $c_0 \leq h\omega \leq C_0$ between h and ω is assumed in Theorem 4.5-Theorem 4.8. As pointed out in Remark 4.1, the condition $h\omega \leq C_0$ is standard for the discretization of Helmholtz equation and time-harmonic Maxwell equations. The assumption $h\omega \geq c_0$ was used in the derivation of the h-convergence orders in Theorem 4.3 (by Lemma 4.1). Although we do not know whether this assumption is absolutely necessary in theory, the numerical results (Figures 1,5,7) in the next section indicate that the $h-$convergence orders of the approximation u_h can be kept without such an assumption (i.e., h decreases but ω is fixed).

As pointed out in [19], it is difficult to obtain an ideal L^2 error estimate of the plane wave approximate solutions of the time-harmonic Maxwell equations. In the present paper we do not investigate L^2 error estimate of the plane wave approximation $\mathbf{E}_h^{(2)}$, but we will report satisfactory L^2 errors of the final approximation $\mathbf{E}_h$ in the next section.

5 Numerical experiments

In this section we apply the PWLS-LSFE method to solve several nonhomogeneous Helmholtz and time-harmonic Maxwell equations, and we report some numerical results to confirm our theoretical results.

We consider Helmholtz equation in two or three dimensions and time-harmonic Maxwell equations in three dimensions. As pointed out in Section 4, we choose $\alpha = \omega^2$ and $\beta = 1$ in the Helmholtz's variational problem (2.7).

For the examples discussed in this section, we consider square or cube domains Ω and we adopt uniform partitions $\mathcal{T}_h$ for the domain Ω as follows. Let Ω be divided into elements Ω_k, which are small cubes (for three-dimensional case) or squares (for two-dimensional case) with an equal length h of a side. As described in Sections 3 and 4, we choose the same number p of basis functions for every elements Ω_k. The resulting discrete systems (3.9) and (3.10) are solved by the direct method.

To measure the accuracy of the numerical solutions u_h and $\mathbf{E}_h$, we introduce the L^2 relative error

$$L^2 \text{ Relat. Err.} := \frac{||u_{ex} - u_h||_{L^2(\Omega)}}{||u_{ex}||_{L^2(\Omega)}}, \quad \text{or} \quad L^2 \text{ Relat. Err.} := \frac{||\mathbf{E}_{ex} - \mathbf{E}_h||_{L^2(\Omega)}}{||\mathbf{E}_{ex}||_{L^2(\Omega)}}$$

for the analytic solution $u_{ex} \in L^2(\Omega)$, or $\mathbf{E}_{ex} \in (L^2(\Omega))^3$.

We perform all computations on a Dell Precision T5500 graphics workstation (2*Intel Xeon X5650 and 6*12GECC) using MATLAB implementations. Here "6*12GECC" means that the Dell Precision T5500 graphics workstation has 6*12G internal memory and adopts the Error Checking and Correcting (ECC) Technology.

5.1 A Helmholtz equation in two dimensions

The first model problem is the Helmholtz equation (2.1), with $\Omega = [0, 1] \times [0, 1]$, and $g = (\frac{\partial}{\partial \mathbf{n}} + i\omega)u_{ex}$. The exact solution of the above problem is defined in the closed form

$$u_{ex}(x, y) = \omega x \ \cos y + y \ \sin(\omega x).$$

Then the source term $f = (\omega^2 - 1)\omega x \ \cos y$.

In order to illustrate the efficiency of the PWLS-LSFE method more clearly, we state the number of elements (and degrees of freedom) per wavelength for the experiments made in this subsection. Let n_e denote the number of elements per wavelength, which is defined by $n_e = \lambda/h = 2\pi/(\omega h)$, and let dof. denote the degrees of freedom per wavelength, i.e., dof.$=n_e p$.

At first we set $\omega = 4\pi$. We fix the number of the plane wave basis functions and the order number of polynomials in the local spectral space as $p = 7, 9$ and $q = 3$, but decrease the mesh size h. The resulting V-norm errors and relative L^2-norm errors of the approximations generated by the PWLS-LSFE method are listed in Table 1 and Fig. 1.

Figure 1 shows the plots of h-convergence orders of the V-norm errors and the relative L^2-norm errors, respectively. The plots highlight regions of high order convergence for decreasing h, which verifies the validity of the theoretical results given

Table 1 Errors of approximations with respect to h ($\omega = 4\pi,\ q = 3$)

	h	$\frac{1}{4}$	$\frac{1}{8}$	$\frac{1}{16}$	$\frac{1}{32}$	$\frac{1}{64}$
$p = 7$	$\|\|u - u_h\|\|_V$	24.569	3.608	5.991e-1	1.047e-1	2.067e-2
	L^2 Relat. Err.	1.110e-1	5.856e-3	3.334e-4	2.041e-5	1.433e-6
	n_e	2	4	8	16	32
	dof.	14	28	56	112	224
$p = 9$	$\|\|u - u_h\|\|_V$	11.026	5.668e−1	3.487e−2	2.475e−3	6.479e−4
	L^2 Relat. Err.	1.279e−1	6.134e−3	3.528e−4	2.156e−5	1.387e−6
	n_e	2	4	8	16	32
	dof.	18	36	72	144	288

in Theorem 4.5 and Theorem 4.6. According to Remark 4.2, the number s defining the h-convergence orders in Theorem 4.5 and Theorem 4.6 is $s = \min\{m+1, q+1\} = 4$, which implies that the V-norm errors and the relative L^2-norm errors respectively have only 2.5-order and 2-order convergence with respect to h (for a fixed ω). Fortunately, the plots indicate that L^2-norm errors possess about 4-order convergence with respect to h, which is obviously superior to the theoretical results. We can see from Fig. 1 that the numerical convergence order in V-norm are almost equal to the theoretical convergence order defined by s for the case of $p = 7$ and $q = 3$. We point out that, for the case of homogeneous equations, the numerical h-convergence order in L^2-norm is also higher than the theoretical h-convergence order (see Remark 4.12 and Remark 4.15 in [15] and the numerical results reported in [21]). Notice that, for sufficiently small h satisfying $\lambda/h > 30$, where the wavelength λ is equal to $2\pi/\omega$, the high convergence orders are still kept.

We can also fix the mesh size h, but increase both p and q. In applications, the mesh size h can be chosen as $h \approx \frac{1}{\omega}$. When ω increases, the parameters p and q also slightly increase such that the resulting approximate solution has some satisfactory

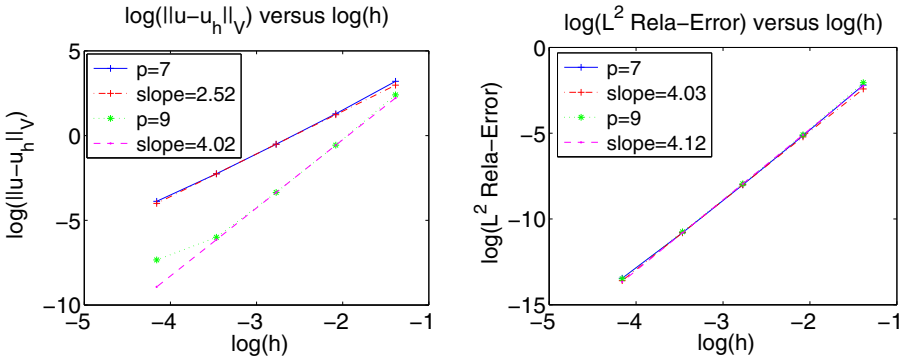

Fig. 1 *Left*: $h-$covergence in V-norm in logarithmic scale. *Right*: $h-$covergence in relative L^2-norm in logarithmic scale

Table 2 Errors of approximations in V-norm with respect to p ($\omega = 4\pi,\ h = 1/12, n_e = 6$)

p	5	7	9	11	13	15
$q = 2$	2.388	1.200	1.246e−1	5.900e−2	3.053e-2	1.353e-2
$q = 3$	2.095	1.249	1.068e−1	5.065e−2	2.877e-2	1.281e-2
$q = 4$	1.714	1.774e−1	2.785e−2	2.017e−2	1.045e-2	6.919e-3
$q = 5$	1.716	1.778e−1	2.362e−2	1.713e−2	9.304e-3	6.148e-3
dof.	30	42	54	66	78	90

accuracy. Here $\omega = 4\pi$, so we can choose h as $h = \frac{1}{12}$. Then the number of elements per wavelength equals 6. The resulting V-norm errors and relative L^2-norm errors of the approximations generated by the PWLS-LSFE method are listed in Tables 2–3 and Figs. 2–3.

It can be seen from Tables 2 and 3 that both the relative L^2-norm errors and the V-norm errors decrease when both p and q increase.

For the L^2-norm errors, balance values of p are $p = p^*(q) = 7$ (rep. 9) when $q = 2, 3$ (rep. $q = 4, 5$), i.e., p^* is an odd number roughly satisfying $p^* \approx 2q + 1$; for the V-norm errors, we can choose the balance value of p as $p^* = 13$ or 15, which is an odd number roughly satisfying $p^* \approx 2q + 5$.

Figure 2 shows the plots of the errors in V-norm with respect to p for different orders q of local polynomials. It can be seen from Fig. 2 that the V-norm errors gradually decrease in a large range of p, so the balance value p^* is not sensitive to q and may not be unique for a fixed q. Moreover, Fig. 2 indicates that the value p^* should not be too large, otherwise, numerical instability prevents us from obtaining the desired accuracy of the approximation (this phenomenon was also observed for the PWDG method and was pointed out in [18]).

When $p \geq p^*$, the L^2-norm errors of u_h are mainly determined by the L^2-norm errors of $u_h^{(1)}$, which are independent of p, so the L^2-norm errors decrease very slowly when p further increases from p^*. Since the L^2-norm errors first rapidly decrease and then decrease very slowly, the balance value p^* for the L^2-norm errors is more important than that for the V-norm errors.

The plots in Fig. 3 display the dependence of the errors of the approximate solutions on the values q for a fixed p. It can be seen from the above figure that

Table 3 Errors of approximations in relative L^2-norm with respect to p ($\omega = 4\pi,\ h = 1/12, n_e = 6$)

p	5	7	9	11
$q = 2$	1.852e-2	8.626e-3	8.601e-3	8.586e-3
$q = 3$	1.899e-2	1.153e-3	1.144e-3	1.138e-3
$q = 4$	1.907e-2	3.064e-4	1.281e-4	1.272e-4
$q = 5$	1.918e−2	3.225e−4	1.276e−4	1.263e−4
dof.	30	42	54	66

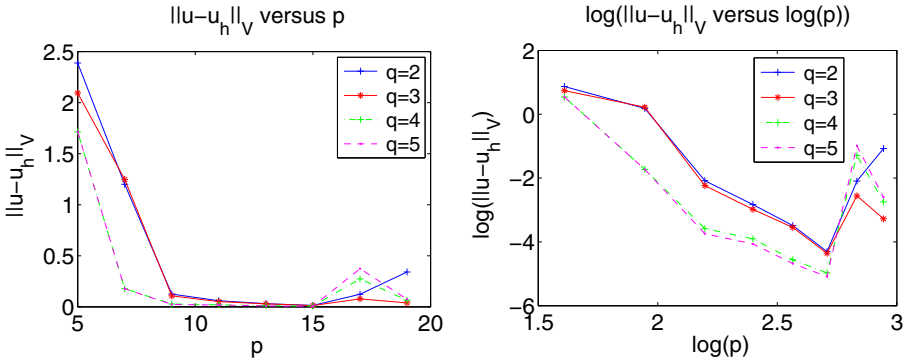

Fig. 2 *Left*: The error in V-norm with respect to p for different orders q of local polynomials. *Right*: The error in V-norm with respect to p for different orders q of local polynomials in logarithmic scale

the relative errors in the L^2 norm decrease faster than the V-norm errors when q increases from 2 to 4 for the cases of $p = 7, 9, 11$. But, when q further increases from 4 to 5 for the case of $p = 5, 7$, the two errors do not decrease yet, since the errors of the plane wave approximations $u_h^{(2)}$ are dominant in the errors of the global approximation u_h. There are interesting phenomenons for the case of $p = 5$: the L^2-norm errors are smaller than the V-norm errors and do not decrease when q increases from 2 to 4, but the V-norm errors decrease when q increases from 2 to 4. These phenomenons indicate that the L^2-norm errors possess higher order convergence of q than the V-norm errors.

Then we consider a larger wave number $\omega = 8\pi$, and investigate the convergence order of the approximate solutions with respect to the mesh size h when we fix p and q. For the choices $p = 13$ and $q = 3$, the corresponding errors are shown in Table 4 and Fig. 4.

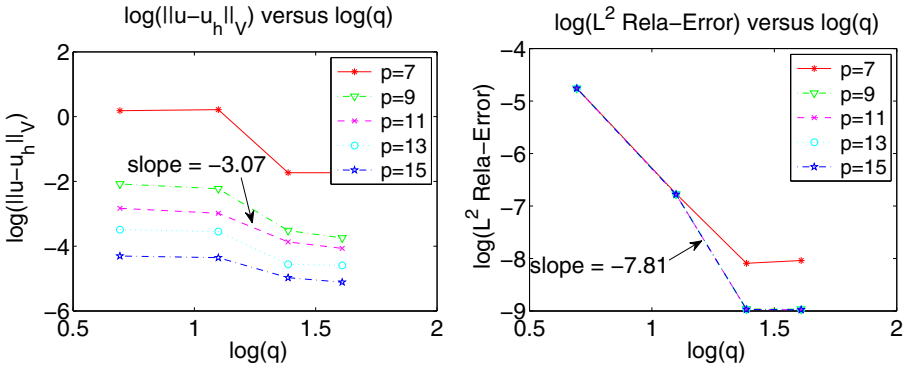

Fig. 3 The errors in V-norm and relative L^2-norm with respect to q for different numbers p of plane wave basis functions in logarithmic scale are plotted

Table 4 Errors of approximations with respect to h ($\omega = 8\pi,\ p = 9,\ q = 3$)

h	$\frac{1}{8}$	$\frac{1}{16}$	$\frac{1}{32}$	$\frac{1}{64}$	$\frac{1}{128}$
$\|\|u - u_h\|\|_V$	51.053	2.502	1.556e-1	1.984e-2	1.185e-3
L^2 Relat. Err.	1.285e-1	6.101e-3	3.515e-4	2.209e-5	2.470e-6
n_e	3	3.5	4	4.5	5
dof.	39	45.5	52	58.5	65

The results listed in Tables 1–3 indicate that the approximations generated by the PWLS-LSFE method possess high accuracy when both p and q increase, or the mesh size h decreases.

Figure 4 shows the plot of $-log(||u - u_h||_V$ and $-log(L^2$ Relat.Err.) with respect to $-log(h)$, respectively. It displays a linear plot, which verifies the validity of the theoretical results given in Theorem 4.6. In fact, the orders of convergence obtained from the plots are superior to the theoretical estimates given in Theorems 4.5 and 4.6.

5.2 A Helmholtz equation in three dimensions

The exact solution of the second model problem is defined in the closed form

$$u_{\text{ex}} = z\ \ \ln(1 + \omega xy), \quad (x, y, z) \in \Omega,$$

where $\Omega = [0, 1] \times [0, 1] \times [0, 1]$.

We set $\omega = 2\pi$ and choose the number p of the plane wave basis functions as $p = 16$. The V-norm errors and the relative L^2-norm errors of the resulting approximations are shown in Table 5 and Fig. 5.

Figure 5 shows the plots of $-log(||u - u_h||_V$ and $-log(L^2$ Relat.Err.) with respect to $-log(h)$, respectively. Similarly to the first test example, it displays a linear plot which verifies the validity of the theoretical results in Theorem 4.5–Theorem 4.6. It can be seen from Table 5 and Fig. 5 that the approximations generated by the

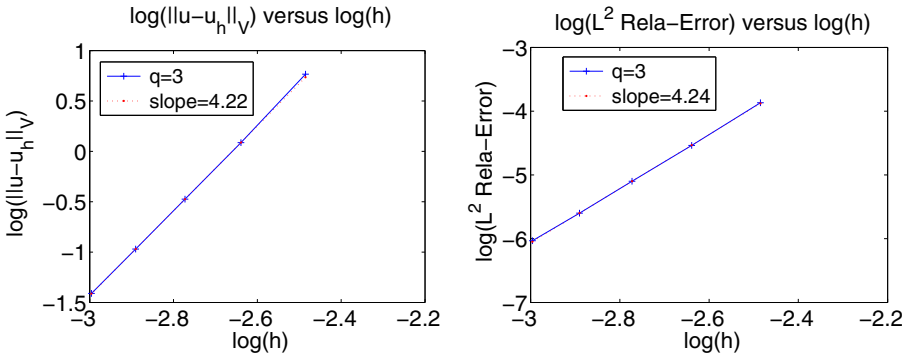

Fig. 4 The errors in V-norm and relative L^2-norm with respect to h in logarithmic scale for different orders q of local polynomials

Table 5 Errors of approximations with respect to h and q ($\omega = 2\pi,\ p = 16$)

	h	$\frac{1}{4}$	$\frac{1}{8}$	$\frac{1}{16}$	$\frac{1}{32}$
$q = 2$	$\|\|u - u_h\|\|_V$	1.717e-1	2.414e-2	3.405e-3	4.846e-4
	L^2 Relat. Err.	1.014e-1	2.325e-2	5.315e-3	1.206e-3
$q = 3$	$\|\|u - u_h\|\|_V$	1.408e-1	2.246e-2	3.711e-3	5.941e-4
	L^2 Relat. Err.	4.794e-2	1.050e-2	2.297e-3	5.257e-4

PWLS-LSFE method with the local space consisting of third order polynomials are more accurate than that generated by the same method with the local space consisting of second order polynomials. Moreover, the convergence orders indicated in the figure are much higher than that obtained by the theoretical results. For example, we investigate the h-convergence orders of the L^2-norm errors for the case of $q = 2$. According to Remark 4.2, the number s in the error estimate (4.24) is equal to $s = \min\{m + 1,\ q + 1\} = 3$ (here $m = 3$), which means that the theoretical convergence order is $s - 2 = 1$ (for a fixed ω). However, the numerical convergence order, i.e., the slope of the line at the bottom row in Fig. 5 is 2.12, which is obviously superior to the theoretical order.

We can also fix the mesh size h as $h = \frac{1}{6}$, but increase both p and q. Here the number of elements per wavelength equals 6. The resulting V-norm errors and relative L^2-norm errors of the approximations generated by the PWLS-LSFE methd are shown in Table 6 and Fig. 6.

It can be seen from Table 6 that both the relative L^2-norm errors and the V-norm errors decrease when both p and q increase in a suitable range. For the L^2-norm errors, the balance values of p are $p = p^*(q) = 16$ (rep. 25) when $q = 2$ (rep. $q = 3$); for the V-norm errors, we can choose the balance value of p as $p^* = 64$.

Similarly to the first example, for a fixed q, the relative L^2-norm errors decrease very slowly when p further increases from p^*.

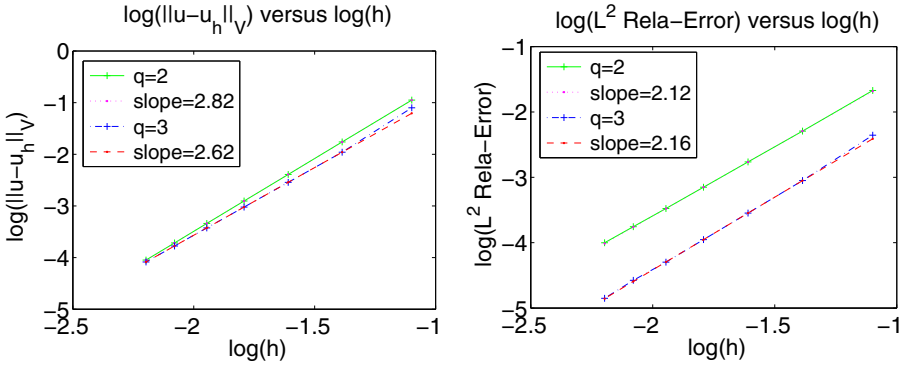

Fig. 5 The errors in V-norm and relative L^2-norm with respect to h in logarithmic scale for different orders q of local polynomials

Table 6 Errors of approximations with respect to p ($\omega = 2\pi,\ h = 1/6$)

	p	16	25	36	49	64
$q = 2$	$\|\|u - u_h\|\|_V$	5.428e-2	1.823e-2	8.965e-3	3.234e-3	1.327e-3
	L^2 Relat. Err.	4.285e-2	4.278e-2	4.276e-2	4.275e-2	4.274e-2
$q = 3$	$\|\|u - u_h\|\|_V$	4.781e-2	8.624e-3	4.946e-3	3.401e-3	1.803e-3
	L^2 Relat. Err.	1.959e-2	1.946e-2	1.945e-2	1.944e-2	1.943e-2

Figure 6 shows the plots of the errors in V-norm with respect to p for different orders q of local polynomials. It can be seen from Fig. 6 that the V-norm errors gradually decrease in a large range of p, so the balance value p^* is not sensitive to q.

Besides, for a fixed p, the L^2-norm errors decrease faster than the V-norm errors when q increases, which indicates that the L^2-norm errors have higher order convergence with respect to q than the V-norm errors.

5.3 An example of Maxwell equations in three dimensions

As pointed out in [22], the PWLS method has an advantage over the other plane wave methods: the PWLS method is a unified method for both non-absorbing medium (i.e., ε is a real number) and absorbing medium (i.e., ε is a complex number), and there is no difference in implementation and convergence of the PWLS method between the two different media. For the other plane wave methods, the discretization of Maxwell equations with absorbing medium is more complicated than that with non-absorbing medium (refer to [23]). In order to reflect this superiority, in this subsection we only consider an example with absorbing medium.

To illustrate the effectiveness of the proposed approach for nonhomogeneous Maxwell equations (2.9), we set $\mu = 1$ and $\varepsilon = 1 + i$ in (2.9). σ is determined

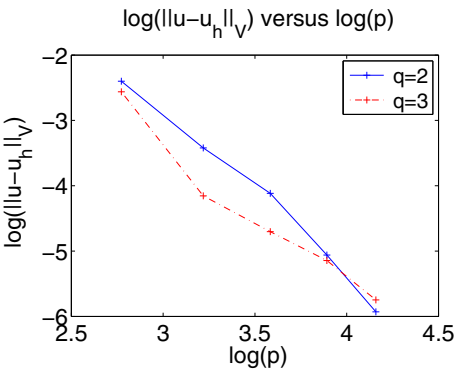

Fig. 6 The error in V-norm with respect to p in logarithmic scale for different orders q of local polynomials

Table 7 Errors of approximations with respect to h ($\omega = 2\pi$, $p = 25$, $q = 2$)

	h	$\frac{1}{4}$	$\frac{1}{6}$	$\frac{1}{8}$
PWLS-LSFE	$\|\|\mathbf{E} - \mathbf{E}_h\|\|_{\mathbf{V}}$	4.371e-1	1.732e-1	9.135e-2
	L^2 Relat. Err.	2.952e-2	1.216e-2	6.417e-3
Method in [22]	$\|\|\mathbf{E} - \mathbf{E}_h\|\|_{\mathbf{V}}$	1.712	1.456	1.353
	L^2 Relat. Err.	1.021e-1	7.569e-2	6.366e-2

by $\sigma = \sqrt{\frac{\mu}{|\varepsilon|}}$ according to the known formula introduced in Ref. [23, Sec. 1]. Considering the following analytical solution

$$\mathbf{E}_{\text{ex}} = \varepsilon\omega(xz\ \cos y, -z\ \sin y, xy)^t, \tag{5.1}$$

where the superscript "t" denote the transpose of a vector. In this example, the source term $\mathbf{J}$ determined by the above solution does not vanish over the entire computational domain $[0, 1]^3$. The discretization of the underlying equations is the same as that of the equations described in Section 3.

As in the previous subsection, we set $\omega = 2\pi$ and choose the number p of the plane wave basis functions as $p = 25$. We first compare the proposed PWLS-LSFE method with the method introduced in [22], here the degree q of polynomials in the local spaces is fixed as $q = 2$. Table 7 shows the V-norm errors and the relative L^2-norm errors of the approximations generated by the two methods. The results listed in Table 7 indicate that the approximations generated by the PWLS-LSFE method indeed have higher accuracy than that generated by the method introduced in [22].

Then we report the results of the PWLS-LSFE methd when h decreases and q increases. Table 8 and Fig. 7 show the V-norm errors and the relative L^2-norm errors of the approximations generated by the proposed method.

The results listed in Table 8 indicate that both V-norm accuracy and L^2-norm accuracy of the approximations generated by the PWLS-LSFE method are satisfactory. Moreover, the approximations associated with third order polynomials in local spectral spaces are more accurate than that associated with second order polynomials in local spectral spaces.

Table 8 Errors of approximations with respect to h and q ($\omega = 2\pi$, $p = 25$)

	h	$\frac{1}{4}$	$\frac{1}{8}$	$\frac{1}{16}$	$\frac{1}{32}$
$q = 2$	$\|\|\mathbf{E} - \mathbf{E}_h\|\|_{\mathbf{V}}$	4.371e-1	9.135e-2	1.913e-2	4.015e-3
	L^2 Relat. Err.	2.952e-2	6.417e-3	1.407e-3	2.998e-4
$q = 3$	$\|\|\mathbf{E} - \mathbf{E}_h\|\|_{\mathbf{V}}$	1.853e-1	2.031e-2	2.312e-3	2.578e-4
	L^2 Relat. Err.	1.133e-2	7.474e-4	4.941e-5	3.268e-6

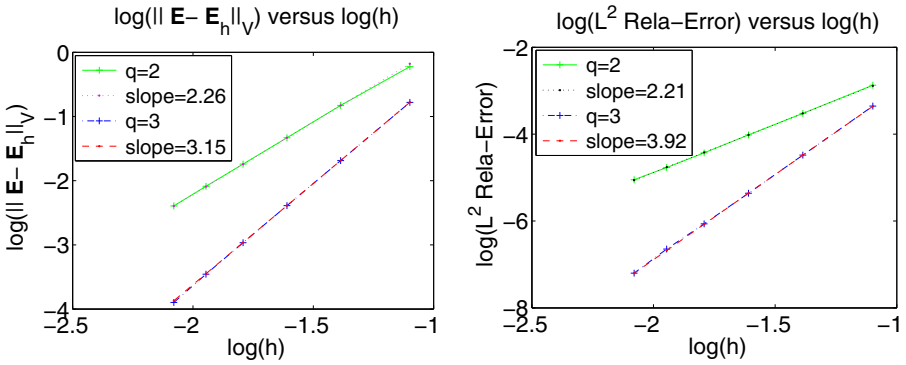

Fig. 7 The errors in V-norm and relative L^2-norm with respect to h in logarithmic scale for different orders q of local polynomials

Figure 7 shows the plot of $-log(||u-u_h||_V$ and $-log(L^2$ Relat.Err.) with respect to $-log(h)$, respectively. It also displays a linear plot which verifies the validity of the theoretical results in Theorem 4.8. As in the second example, the numerical convergence orders indicated in the plots are superior to the theoretical ones from the Theorem 4.8.

We can also fix the mesh size h as $h = \frac{1}{5}$, but increase both p and q. Here the number of elements per wavelength equals 5. The resulting V-norm errors and relative L^2-norm errors of the approximations generated by the PWLS-LSFE methd are listed in Table 9 and Fig. 8.

It can be seen from Table 9 that both the relative L^2-norm errors and the V-norm errors decrease when both p and q increase in a suitable range. For the L^2-norm errors, the balance values of p are $p = p^*(q) = 16$ (rep. 25) when $q = 2$ (rep. $q = 3$); for the V-norm errors, we can choose the balance value of p as $p^* = 64$. Similarly to the previous two examples, for a fixed q, the L^2-norm errors decrease very slowly when p further increases from p^*; while, for a fixed p, the L^2-norm errors decrease faster than the V-norm errors when q increases.

Figure 8 shows the plots of the errors in V-norm with respect to p for different orders q of local polynomials. It can be seen from Fig. 8 that the V-norm errors gradually decrease in a large range of p, so the balance value p^* is not sensitive to q.

Table 9 Errors of approximations with respect to p ($\omega = 2\pi,\ h = 1/5$)

	p	16	25	36	49	64
$q = 2$	$\|\|\mathbf{E} - \mathbf{E}_h\|\|_{\mathbf{V}}$	3.505e-1	2.651e-1	2.216e-1	1.041e-1	7.079e-2
	L^2 Relat. Err.	1.804e-2	1.800e-2	1.842e-2	1.855e-2	1.944e-2
$q = 3$	$\|\|\mathbf{E} - \mathbf{E}_h\|\|_{\mathbf{V}}$	2.612e-1	9.173e-2	2.151e-2	1.849e-2	1.475e-2
	L^2 Relat. Err.	5.363e-3	4.706e-3	5.992e-3	6.994e-3	8.441e-3

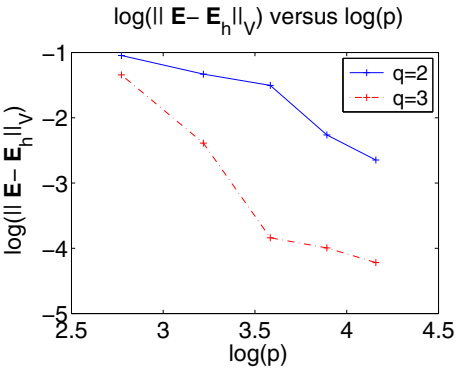

Fig. 8 The error in V-norm with respect to p in logarithmic scale for different orders q of local polynomials

6 Conclusion

In this paper we have introduced a plane wave method combined with local spectral elements for the discretization of nonhomogeneous Helmholtz equation and time-harmonic Maxwell equations and derived error estimates of the resulting approximate solutions. The error estimates show that the approximate solutions generated by the new method possess high accuracy. We reported some numerical results to illustrate the theoretical results.

Acknowledgments The authors wish to thank the anonymous referee for many insightful comments which led to great improvement in the results and the presentation of the paper.

References

1. Amara, M., Djellouli, R., Farhat, C.: Convergence analysis of a discontinuous Galerkin method with plane waves and Lagrange multipliers for the solution of Helmholtz problems. SIAM J. Numer. Anal. **47**, 1038–1066 (2009)
2. Alves, C., Chen, C.: A new method of fundamental solutions applied to nonhomogeneous elliptic problems. Adv. Comput. Math. **23**, 125–142 (2005)
3. Alves, C., Valtchev, S.: Numerical comparison of two meshfree methods for acoustic wave scattering. Eng. Anal. Bound. Elem. **29**, 371–382 (2005)
4. Brenner, S., Scott, L.: Mathematical Theory of Finite Element Methods, 3Rded., Texts Appl. Math. Springer, New York (2002)
5. Buffa, A., Monk, P.: Error estimates for the ultra weak variational formulation of the Helmholtz equation. ESAIM: M2AN Math. Model. Numer. Anal. **42**, 925–940 (2008)
6. Cessenat, O.: Application d'une nouvelle formulation variationnelle aux équations d'ondes harmoniques, Problèmes de Helmholtz 2D et de Maxwell 3D, Ph.d. thesis, Université Paris IX Dauphine (1996)
7. Cessenat, O., Despres, B.: Application of an ultra weak variational formulation of elliptic PDEs to the two-dimensional Helmholtz problem. SIAM J. Numer. Anal. **35**, 255–299 (1998)
8. Cessenat, O., Despres, B.: Using plane waves as basis functions for solving time Harmonic equations with the ultra weak variational formulation. J. Comput. Acous. **11**, 227–238 (2003)
9. Deckers, E., Atak, O., Coox, L., DAmico, R., Devriendt, H., Jonckheere, S., Koo, K., Pluymers, B., Vandepitte, D., Desmet, W.: The wave based method: an overview of 15 years of research. Wave Motion **51**, 550–565 (2014)

10. Desmet, W.: A wave based prediction technique for coupled vibro-acoustic analysis. KULeuven, Division PMA, Ph.D. Thesis 98D12 (1998)
11. Du, Y., Wu, H.: Preasymptotic error analysis of higher order FEM and CIP-FEM for Helmholtz equation with high wave number. SIAM J. Numer. Anal. **53**(2), 782–804 (2015)
12. Farhat, C., Tezaur, R., Toivanen, J.: A domain decomposition method for discontinuous Galerkin discretizations of Helmholtz problems with plane waves and Lagrange multipliers. Int. J. Numer. Methods Eng. **78**(13), 1513–1531 (2009)
13. Feng, X., Wu, H.: Hp-discontinuous Galerkin methods for the Helmholtz equation with large wave number. Math. Comp. **80**(276), 1997–2024 (2011)
14. Gabard, G.: Discontinuous Galerkin methods with plane waves for time-harmonic problems. J. Comput. Phys. **225**, 1961–1984 (2007)
15. Gittelson, C., Hiptmair, R., Perugia, I.: Plane wave discontinuous Galerkin methods: analysis of the *h*-version. ESAIM Math. Model. Numer. Anal. **43**, 297–331 (2009)
16. Guo, B., Sun, W.: The optimal convergence of the h-p version of the finite element method with quasi-uniform meshes. SIAM J. Numer. Anal. **45**, 698–730 (2007)
17. Hetmaniuk, U.: Stability estimates for a class of Helmholtz problems. Commun. Math. Sci. **5**, 665–678 (2007)
18. Hiptmair, R., Moiola, A., Perugia, I.: Plane wave discontinuous Galerkin methods for the 2D Helmholtz equation: analysis of the *p*-version. SIAM J. Numer. Anal. **49**(1), 264–284 (2011)
19. Hiptmair, R., Moiola, A., Perugia, I.: Error analysis of Trefftz-discontinuous Galerkin methods for the time-harmonic Maxwell equations. Math. Comp. **82**, 247–268 (2013)
20. Howartha, C., Childs B, P., Moiola, A.: Implementation of an interior point source in the ultra weak variational formulation through source extraction. J. Comput. Appl. Math. **271**, 295–306 (2014)
21. Hu, Q., Yuan, L.: A weighted variational formulation based on plane wave basis for discretization of Helmholtz equations. Int. J. Numer. Anal. Model. **11**, 587–607 (2014)
22. Hu, Q., Yuan, L.: A plane wave least-squares method for time-harmonic Maxwell's equations in absorbing media. SIAM J. Sci. Comput. **36**, A1911–A1936 (2014)
23. Huttunen, T., Malinen, M., Monk, P.: Solving Maxwell's equations using the ultra weak variational formulation. J. Comput. Phys. **223**, 731–758 (2007)
24. Moiola, A., Hiptmair, R., Perugia, I.: Plane wave approximation of homogeneous Helmholtz solutions. Z. Angew. Math. Phys. **62**, 809–837 (2011)
25. Monk, P.: Finite Element Methods for Maxwell's Equation. Oxford University Press (2003)
26. Monk, P., Wang, D.: A least-squares method for the Helmholtz equation. Comput. Methods Appl. Mech. Engrg. **175**, 121–136 (1999)
27. Riou, H., Ladevèze, P., Sourcis, B.: The multiscale VTCR approach applied to acoustics problems. J. Comput. Acous. **16**, 487–505 (2008)
28. Riou, H., Ladevèze, P., Sourcis, B., Faverjon, B., Kovalevsky, L.: An adaptive numerical strategy for the medium-frequency analysis of helmholtz's problem. J. Comput. Acous. **20**(1) (2012)
29. Sloane, N.: Tables of spherical codes, http://neilsloane.com/packings/dim3 (2014)
30. Tezaur, R., Farhat, C.: Three-dimensional directional discontinuous Galerkin elements with plane waves and lagrange multipliers for the solution of mid-frequency Helmholtz problems. Int. J. Numer. Meth. Engng. **66**(5), 796–815 (2006)
31. Trefftz, E.: Ein gegenstuck zum ritzschen verfahren. Sec. Inte. Cong. Appl. Mech., 131–137 (1926)